1   # Bacterial lifestyle switch in response to algal metabolites

2   Noa Barak-Gavish[1], Bareket Dassa[2], Constanze Kuhlisch[1], Inbal Nussbaum[1], Gili Rosenberg[3],
3   Roi Avraham[3] and Assaf Vardi[1*]

4   [1]Department of Plant and Environmental Sciences, [2]Bioinformatics Unit, Department of Life
5   Sciences Core Facilities and [3]Department of Biological Regulation, Weizmann Institute of
6   Science, Rehovot 7610001, Israel.

7   *Corresponding author: Assaf Vardi
8   **Email:** assaf.vardi@weizmann.ac.il

9   **Author Contributions:** N.B.G and A.V. conceptualized the research questions and hypotheses,
10   designed the experiments and wrote the manuscript. N.B.G. preformed all experiments and
11   analyzed the data. N.B.G. and B.D. performed bioinformatics analyses. B.D. G.R. and R.A. took
12   part in the transcriptome experimental design and contributed to scientific discussions. C.K.
13   performed benzoate measurements. I.N. assisted in laboratory experiments.

14   **Competing Interest Statement:** The authors declare that they have no competing interests.

15   **Classification:** Major: Biological Sciences, Minor: Microbiology.

16   **Keywords:** Chemical communication, Phytoplankton, Roseobacter, DMSP, Benzoate.

17   **This PDF file includes:**
18   Main Text
19   Figures 1 to 6

Abstract

20

21 Unicellular algae, termed phytoplankton, greatly impact the marine environment by serving as the

22 basis of marine food webs and by playing central roles in biogeochemical cycling of elements. The

23 interactions between phytoplankton and heterotrophic bacteria affect the fitness of both partners.

24 It is becoming increasingly recognized that metabolic exchange determines the nature of such

25 interactions, but the underlying molecular mechanisms remain underexplored. Here, we

26 investigated the molecular and metabolic basis for the bacterial lifestyle switch, from coexistence

27 to pathogenicity, in *Sulfitobacter* D7 during its interaction with *Emiliania huxleyi*, a cosmopolitan

28 bloom-forming phytoplankter. To unravel the bacterial lifestyle switch, we profiled bacterial

29 transcriptomes in response to infochemicals derived from algae in exponential and stationary

30 growth, which induced the *Sulfitobacter* D7 coexistence and pathogenicity lifestyles, respectively.

31 We found that algal dimethylsulfoniopropionate (DMSP) was a pivotal signaling molecule that

32 mediated the transition between the lifestyles. However, the coexisting and pathogenic lifestyles

33 were evident only in the presence of additional algal metabolites. In the pathogenic mode,

34 *Sulfitobacter* D7 upregulated flagellar motility and many transport systems, presumably to

35 maximize assimilation of *E. huxleyi*-derived metabolites released by algal cells upon cell death.

36 Specifically, we discovered that algae-produced benzoate promoted the growth of *Sulfitobacter* D7,

37 and negated the DMSP-inducing lifestyle switch to pathogenicity, demonstrating that benzoate is

38 important for maintaining the coexistence of algae and bacteria. We propose that bacteria can

39 sense the physiological status of the algal host through changes in the metabolic composition,

40 which will determine the bacterial lifestyle during the interactions.

Significance Statement

41

42 Microorganisms in the marine environment play crucial roles in the regulation of Earth's climate

43 and elemental cycling. Understanding microbial interactions and the metabolic exchange that

44 drives them is necessary for disentangling the complexity of the marine ecosystem. Here we

45 demonstrate how the opportunistic pathogen *Sulfitobacter* D7 switches its lifestyle from

46 coexistence to pathogenicity in response to metabolites released by *Emiliania huxleyi*, a bloom-

47 forming unicellular alga. By mapping bacterial transcriptional profiles, we show that the algal

48 metabolite dimethylsulfoniopropionate (DMSP), an important signaling molecule in the marine

49 environment, is essential for the bacterial lifestyle switch. However, the activity of DMSP depended

50 on additional algal signals. This work emphasizes how metabolic crosstalk can influence the nature

51 and fate of microbial interactions, which have cascading effects on large-scale oceanic processes.

Main Text

Introduction

Half of Earth's photosynthesis occurs in the marine environment by phytoplankton – photosynthetic single-celled algae (1). Phytoplankton have great ecological importance by forming the basis of marine food webs and influencing biogeochemical cycles. Therefore, the biotic interactions phytoplankton engage in, and the metabolic exchange that govern them, have immense impacts on large-scale biogeochemical processes. Phytoplankton are a main source of organic matter in the marine environment thus fueling the growth and function of heterotrophic bacteria that interact with them through chemical exchange (2, 3). Although the marine environment is characterized by its diluted and turbulent nature, efficient chemical communication takes place in the phycosphere – the diffusive boundary layer that surrounds algal cells, where molecules can accumulate to high concentrations (2, 4). Studies on algae-bacteria interactions revealed that the partners often exchange growth substrates (5, 6), essential vitamins and nutrients (7–9), and infochemicals (molecules that convey information) (10–13). Bacteria have developed mechanisms, such as motility and chemotaxis, for foraging of phytoplankton cells and attachment to their surfaces to maintain close association within the phycosphere (14–21).

Bacteria from the *Rhodobacterales* order, often termed Roseobacters, are found to be associated with phytoplankton (22–29). They are metabolically versatile and specialize on algae-derived substrates that promote interactions with phytoplankton (30). The organosulfur molecule dimethylsulfoniopropionate (DMSP), produced by many phytoplankton species (31), is especially known to mediate Roseobacter-phytoplankton interactions by serving as a carbon and sulfur source, a chemotaxis cue and as an infochemical for the presence of algae (5, 12, 13, 32–36). In mutualistic interactions algae provide organic matter such as sugars, amino acids, sulfonates and polyamines for bacterial growth. In exchange, Roseobacters often produce essential B-vitamins and growth promoting factors such as indole-3-acetic acid (IAA) (5, 12, 37, 38). In recent years cumulating studies that investigated the interactions of phytoplankton and bacteria in co-cultures revealed that some Roseobacters display a lifestyle switch from mutualism to pathogenicity towards the algae. This occurs when the algal host reaches stationary growth and is mediated by infochemicals (6, 7, 13, 39–41). For example, Roseobacters can produce potent algicidal compounds, termed roseobacticides, in response to *p*-coumaric acid, an aromatic lignin breakdown product released by aging algae (11, 34). While this bacterial lifestyle switch, often termed the "Jekyll-and-Hyde" phenotype, seems to be a recurring phenomenon, knowledge about the bacterial behavior in the different modes of interaction and the regulation of such lifestyle switch is still rudimentary.

86   In the current study we investigated the behavior of the Roseobacter *Sulfitobacter* D7, during

87   interactions with *Emiliania huxleyi*, a cosmopolitan bloom-forming phytoplankter. *E. huxleyi* has a

88   central role in biogeochemical cycling of carbon and sulfur. It produces the climatically active gas

89   dimethyl sulfide and its precursor DMSP, both act as infochemicals during interactions with *E.*

90   *huxleyi* (13, 42). *Sulfitobacter* sp. are associated with *E. huxleyi* in nature, and *Sulfitobacter* D7 was

91   isolated from a natural *E. huxleyi* bloom (13, 28, 43, 44). Therefore, this ecologically-relevant model

92   provides a tractable system to examine how metabolic exchange regulates the nature of

93   interactions between algae and bacteria. Our previous work revealed that *Sulfitobacter* D7 displays

94   a lifestyle switch, from coexistence to pathogenicity, during its interaction with *E. huxleyi*. We found

95   that algal DMSP, which usually mediates mutualistic interactions, plays a pivotal role by invoking

96   bacterial pathogenicity (13). Many studies investigated the genes related to DMSP uptake and

97   catabolism (45–49), but the regulation and molecular basis of DMSP-responsive genes and how

98   these affect bacterial lifestyle and behavior during interactions with algae are yet to be explored.

99   We performed a transcriptome experiment that allowed us to elucidate the bacterial response to

100   algal infochemicals, and to characterize DMSP-responsive and pathogenicity-related genes. We

101   revealed the signaling role of DMSP that leads to systemic remodeling of *Sulfitobacter* D7 gene

102   expression, but only in the presence of additional algal metabolites. Overall, we unravel the

103   transcriptional signature of the shift from coexistence to pathogenic bacterial lifestyles during

104   interactions with their algal host and provide insights into the ecological context of these modes of

105   interactions.

106

Results

108   ### *E. huxleyi*-derived exudates induce remodeling of *Sulfitobacter* D7 transcriptome

109   The interaction between *Sulfitobacter* D7 and *E. huxleyi* displays two distinct phases (Fig.

110   1a). Initially, there is a coexisting phase in which the alga grows exponentially and the bacterium

111   grows as well. The interaction shifts to pathogenic when the virulence of *Sulfitobacter* D7 towards

112   *E. huxleyi* is invoked upon exposure to high concentrations of algal DMSP, which occurs when the

113   algae reach stationary growth or when DMSP is applied exogenously to algae in exponential growth

114   (Fig. 1a) (13). We aimed to unravel the response of *Sulfitobacter* D7 to the pathogenicity-inducing

115   compound, DMSP, and to different algae-derived infochemicals that affect the lifestyle of the

116   bacterium. We grew *Sulfitobacter* D7 in conditioned media (CM) derived from algal cultures at

117   exponential and stationary phase (Exp-CM and Stat-CM, respectively), in which DMSP

118   concentration is low and high, respectively (13) (Fig. 1b, Table S1). This enabled us to dissect the

119   interaction with *E. huxleyi* into its different phases, i.e., Exp-CM represents the coexisting phase,

120   and Stat-CM represents the pathogenic phase. An additional pathogenicity-inducing treatment was

121   Exp-CM supplemented with 100 μM DMSP (herein Exp-CM+DMSP). This condition mimicked co-

122   cultures to which we added DMSP exogenously and thus induced *Sulfitobacter* D7 pathogenicity,

123   which lead to death of exponentially growing *E. huxleyi*. In order to reveal the bacterial

124   transcriptional response to algal exudates, we harvested bacterial cells after 24 h of growth in the

125   different CM treatments and performed RNAseq analysis, using a modified protocol based on

126   Avraham *et al.*, 2016 (50) (Fig. 1b, Table S1). We aimed to identify pathogenicity-related genes by

127   comparing *Sulfitobacter* D7 gene expression profiles in the pathogenicity-inducing media to the

128   coexistence medium. We also aimed to identify bacterial genes that are specifically responsive to

129   DMSP, and are not affected by other algae-derived factors. Therefore, we grew *Sulfitobacter* D7 in

130   defined minimal medium (MM), which lacks algal metabolites, supplemented it with 100 µM DMSP

131   (herein MM+DMSP), and examined the transcriptional response. This experimental design allowed

132   us to expand our understanding on the bacterial response to DMSP, algal infochemicals and which

133   of these are essential for coexistence and pathogenicity.

134   Among the 3803 genes in *Sulfitobacter* D7 genome, we detected 2588 genes (Table S2).

135   Principle component analysis (PCA), based on the expression profile of all the detected genes,

136   showed a clear separation between the different CM treatments, while the MM ± DMSP samples

137   clustered together (Fig. 1c). Pearson correlation between all samples indicated high correlation

138   between the triplicates of each treatment and hierarchical clustering showed that MM samples

139   cluster separately from the CM samples (Fig. S1). Among the CM samples, Stat-CM and Exp-

140   CM+DMSP were closer and had high correlation to each other compared to Exp-CM (Fig. S1). This

141   suggests that the pathogenicity-inducing impact of the former media is mediated by a unique set of

142   expressed genes, distinct from that induced by the coexistence medium.

143   In order to identify the pathogenicity- and DMSP-related genes we examined the genes

144   that were differentially expressed (DE) in the following comparisons: Exp-CM+DMSP vs. Exp-CM,

145   Stat-CM vs. Exp-CM and MM+DMSP vs. MM. We defined significantly DE genes as |fold change|>2

146   and adjusted *P*-value ≤ 0.05. The DE genes were separated into 4 clusters, based on k-means

147   clustering, and we assessed the enrichment in KEGG pathways in each cluster (Fig. 1d). Cluster 1

148   contained genes that were responsive to DMSP, namely DE in Exp-CM±DMSP and in MM±DMSP

149   comparisons. Interestingly, the expression pattern of cluster 1 genes in response to DMSP was

150   largely different: in Exp-CM, DMSP lead to downregulation, while in MM it lead to upregulation. The

151   differential effect of DMSP in Exp-CM and MM is also visualized in the PCA and is evident by the

152   number of DE genes in the comparisons: 968 genes were DE between Exp-CM vs. Exp-

153   CM+DMSP, while only 170 genes were DE between MM vs. MM+DMSP (Table S3). Since the

154   metabolic composition of these two media was profoundly different, it suggests that the effect of

155   DMSP signaling depends also on the chemical environment. Namely, in different chemical contexts

156   DMSP will affect *Sulfitobacter* D7 gene expression in a different way.

157   Cluster 2 contained genes that were highly expressed in the coexistence medium, Exp-
158   CM, compared to the pathogenicity-inducing media, therefore, we consider it as coexistence-
159   related. This cluster was enriched with genes related to the phenylalanine metabolism pathway,
160   and specifically to phenylacetic acid (PAA) degradation (Table S4). PAA is a phytohormone that
161   can potentially promote algal growth (51), and PAA metabolism by bacteria is related to production
162   of secondary metabolites that can affect algae (52, 53). Clusters 3 and 4 contained genes that were
163   mainly upregulated in Exp-CM+DMSP and Stat-CM compared to Exp-CM, and we consider these
164   as pathogenicity-related clusters. Cluster 4 also contained genes that were expressed in
165   MM±DMSP. Cluster 3 was enriched with genes encoding for ABC transporters and ribosomal
166   proteins, and cluster 4 was enriched with flagellar genes and genes related to oxidative
167   phosphorylation (Fig. 1d, Table S4). The enrichment in genes encoding for ribosomal proteins and
168   an F-type ATPase, related to oxidative phosphorylation, in the pathogenicity-related clusters
169   suggests that during the pathogenic lifestyle *Sulfitobacter* D7 is more metabolically active than in
170   the coexistence lifestyle (Table S4). Overall, this transcriptome experimental setup enabled us to
171   capture the gene expression of *Sulfitobacter* D7 in coexistence and pathogenicity modes.
172   Moreover, it demonstrated the pivotal role of DMSP in regulating gene expression in a context-
173   dependent manner. In *E. huxleyi*-derived CM, DMSP led to major changes in *Sulfitobacter* D7
174   transcriptome, while in MM, which lacked additional algal metabolites, DMSP had a minor effect on
175   gene expression. We therefore suggest that the additional algal factors act in concert with DMSP
176   and are required for the expression of coexistence- and pathogenicity-related genes.

177

178   **The pathogenic lifestyle of *Sulfitobacter* D7 includes upregulation of flagellar genes and**
179   **increased motility**
180   The enrichment in flagellar genes in cluster 4 suggests that flagellar motility may be
181   involved in the pathogenic lifestyle of *Sulfitobacter* D7. We examined the expression of all the genes
182   necessary for flagellar assembly, which are organized in an operon-like structure in *Sulfitobacter*
183   D7 genome (Fig. 2a). Most of the flagellar genes were significantly upregulated in pathogenicity-
184   inducing media compared to the coexistence medium (Fig. 2a). This includes the majority of the
185   genes encoding for the flagellar hook and basal body (Fig. 2a and Table S5). The genes FliC, FliM,
186   FlgC, FlgB and FliI were not DE but were highly expressed in all treatments (Table S5). The genes
187   FlhB, FliR, FlhA and FliQ were not sufficiently detected in our analysis. In MM, however, there were
188   no significant changes in expression of flagellar genes in response to DMSP, although the overall
189   expression was higher than in the CM samples (Fig. 2a, Table S5).

190   To assess the involvement of motility in the behavioral switch of *Sulfitobacter* D7 and to
191   validate the expression patterns of flagellar genes, we performed a functional bacterial motility
192   assay in response to *E. huxleyi*-derived metabolites. We examined the colony expansion of
193   *Sulfitobacter* D7 in semi-solid agar plates composed of Exp-CM, Exp-CM+DMSP or Stat-CM. We
194   first pre-conditioned *Sulfitobacter* D7 in the respective liquid CM for 24 h, in order to induce the
195   appropriate expression of flagellar genes. *Sulfitobacter* D7 plated on pathogenicity-inducing semi-
196   solid media showed higher colony expansion area than in the coexistence medium, indicating
197   increased motility in these conditions (Fig. 2 b-c). The average colony area in semi-solid Stat-CM
198   and Exp-CM+DMSP was 37 and 20.8 mm^2, respectively, while in Exp-CM it was only 13 mm^2 (Fig.
199   2b). Moreover, the morphology of the colonies was different; the colony edges in Stat-CM were
200   smeared and there were bacterial motility extensions from the core colony, indicating bacterial
201   migration in the semi-solid agar (Fig. 2c). The smeared edges were also evident in Exp-CM+DMSP,
202   but to a lesser extent. These results validated the expression patterns of flagellar genes in each
203   CM. Interestingly, *Sulfitobacter* D7 that was pre-grown in liquid marine broth (½MB), and was
204   therefore not pre-exposed to *E. huxleyi* infochemicals, and subsequently plated on the three semi-
205   solid CM did not show major differences in the average colony area. This strongly indicates that
206   *Sulfitobacter* D7 grown in liquid pathogenicity-inducing media were pre-conditioned for motility by
207   upregulating the expression of flagellar genes compared to the coexistence medium. Nevertheless,
208   colonies plated on Stat-CM were significantly larger and showed the smeared edges morphology,
209   implying that in semi-solid Stat-CM there was also induction of motility. Taken together, high
210   expression of flagellar genes in pathogenicity-inducing media, along with the observation that
211   bacteria are indeed more motile in these conditions, indicate that flagella-driven motility may be
212   involved in the pathogenic lifestyle of *Sulfitobacter* D7 during interaction with *E. huxleyi*.

213

214   DMSP and *E. huxleyi*-derived metabolites modulate the expression of *Sulfitobacter* D7
215   transport genes

216   The enrichment in ABC transporters in cluster 3 suggests that nutrient uptake by
217   *Sulfitobacter* D7 is prominent during the interaction with *E. huxleyi*. We examined the expression
218   of all 493 transport genes in *Sulfitobacter* D7 genome. We found that transporters for energy-rich
219   organic compounds were expressed in CM treatments (Fig. 3, Table S6). This includes transporters
220   for amino acids and peptides, carbohydrates and sugars, organic sulfur and nitrogen compounds,
221   as well as for inorganic nutrients and metals. Examination of bacterial transport genes was shown
222   to serve as a sensitive readout for estimating which metabolites reside in the media and are taken
223   up by bacteria (54). Therefore, the expression of transporters implies that the CM contained *E.*
224   *huxleyi*-derived metabolites that *Sulfitobacter* D7 can benefit from during growth in CM and during

7

225   the interaction with the alga. Such metabolites include branched-chain amino acids, sugars, C4

226   carbohydrates and DMSP, which are known to be produced by *E. huxleyi* (55, 56) (Fig. 3).

227   Numerous transport genes were DE in the pairwise comparisons of the different treatments

228   (Fig. 3, Fig. S2 and Table S6). *Sulfitobacter* D7 grown in Stat-CM had a similar expression profile

229   of transport genes to that of Exp-CM+DMSP (Fig. 3, Fig. S2 and Table S6). Therefore, *Sulfitobacter*

230   D7 grown in the pathogenicity-inducing media was indeed in a unique transcriptional and metabolic

231   state compared to the coexistence medium. Many transport genes were mostly upregulated in Exp-

232   CM+DMSP compared to Exp-CM: 99 genes, which constitute ~20% of *Sulfitobacter* D7 transport

233   genes (Fig. 3, Fig. S2). An additional 39 genes were downregulated in response to DMSP addition

234   to Exp-CM. Interestingly, also in MM+DMSP 42 transport genes were upregulated compared to

235   MM, and 14 were downregulated. Namely, in both Exp-CM and MM, DMSP induced remodeling of

236   the transporter repertoire. The fact that the addition of a single metabolite, i.e. DMSP, lead to DE

237   of a multitude of transporters for various metabolite classes demonstrates the signaling role of

238   DMSP. When we examined the amount of DE transport genes that were shared between the

239   comparisons of the DMSP-added samples, we found only 8 genes were differentially expressed in

240   a similar manner (Fig. S2). Namely, DMSP lead to a shift in transporter gene expression in both

241   media but the identity of the DE transporters was unique for each media. This strengthens our

242   hypothesis that the DMSP signal affects bacterial gene expression but the activation of coexistence

243   and pathogenic transcriptional profile depends also on additional algal factors.

244   The differential effect of DMSP in Exp-CM and MM was especially notable in the

245   expression of the DMSP transporters (BCCT, betaine-carnitine-choline transporter), which were

246   significantly upregulated in Stat-CM and Exp-CM+DMSP, where DMSP was present at high

247   concentrations, compared to Exp-CM. However, the expression of these transporters was not

248   affected by the addition of DMSP in the MM±DMSP treatments. This was the same for the *DmdA*

249   gene that encodes for the enzyme responsible for the first step of DMSP breakdown (49) (Table

250   S7). *DmdA* was barely expressed in MM+DMSP, albeit DMSP was present in high concentrations.

251   Therefore, DMSP uptake and metabolism were prominent in *E. huxleyi*-derived CM, which contain

252   additional algal factors that are not present in MM. Taken together, it seems that DMSP has a

253   strong signaling role, however, additional algal components are required to induce the coexistence-

254   to pathogenicity-related gene expression in *Sulfitobacter* D7.

255

256   **Algal benzoate is a key metabolite for *E. huxleyi-Sulfitobacter* D7 coexistence**

257   We searched in the *Sulfitobacter* D7 transcriptomic response to *E. huxleyi*-derived

258   metabolites for evidence of involvement of additional algal factors, other than DMSP, in the

259 regulation of the lifestyle switch from coexistence to pathogenicity. We revealed a plasmid-encoded
260 degradation pathway of the aromatic compound benzoate that was highly expressed in CM
261 samples (Fig. 4a-b, Table S8). Aromatic compound degradation is a common metabolic feature in
262 Roseobacters (57, 58). The metabolic intermediates of benzoate catabolism can be directed to β-
263 ketoadipate, which is subsequently metabolized to form the TCA precursors acetyl-CoA and
264 succinate (59). There are two pathways to metabolize benzoate to β-ketoadipate, through catheol
265 (*Ben* genes) and through 4-hydroxybenzoate and protocatecuate (*BphA* and *PobA* genes) (Fig.
266 S3). An additional benzoate degradation pathway is through benzoyl-CoA (*Box* genes) (Fig. S3)
267 (60). *Sulfitobacter* D7 harbors the pathway through catechol (Fig. 4a). The *Ben* genes are
268 organized in an operon-like structure adjacent to a transcription factor *BenM*, which is known to
269 regulate the expression of *BenABCD* and *CatAB* (Fig 4b) (61, 62). All the genes in this benzoate-
270 degradation operon were expressed in CM treatments. Interestingly, the transporter of benzoate,
271 which is encoded by a chromosomal gene, was also expressed in all CM, therefore it is not affected
272 by the DMSP signal, as was observed for other transport systems (Fig. 3b). This suggest that
273 *Sulfitobacter* D7 can assimilate and perceive algae-derived benzoate as a growth factor or signal
274 regardless of the concentration of DMSP and may therefore be important in the initial coexistence
275 phase.

276   To test if *Sulfitobacter* D7 can grow and metabolize benzoate we inoculated the bacterium
277 in MM supplemented with 100 μM benzoate as a sole carbon source. *Sulfitobacter* D7 grew by 3
278 orders of magnitude within 24h and consumed benzoate to an undetectable level, while the
279 concentration of benzoate in the non-inoculated medium did not change significantly (Fig. 4c). We
280 also detected benzoate in the media of exponentially growing *E. huxleyi* cultures (Fig. S4). This
281 suggests that *Sulfitobacter* D7 can grow on benzoate and benefit from this metabolite during
282 interactions with *E. huxleyi*.

283   Bacterial degradation of various aromatic compounds is mostly directed to the β-
284 ketoadipate pathway and eventually to the TCA cycle (59). While this pathway seems to exist in
285 many Roseobacters, the direct degradation of benzoate is limited to only few species (30, 57). We
286 examined the prevalence of benzoate degradation and transport genes among phytoplankton-
287 associated bacteria. Specifically, we searched for benzoate transporters and genes that directly
288 metabolize benzoate through one of the three possible pathways (Fig. S3, Table S9 and S10). We
289 found that in addition to *Sulfitobacter* D7 another *Sulfitobacter* sp., CB2047, which was also isolated
290 from an *E. huxleyi* bloom (44), was able to utilize benzoate, namely, its genome encodes for both
291 degradation and transport genes (Fig. 3d). We found indications for benzoate utilization in the
292 genomes of two additional *Roseobacter*s, *Rhodobacteraceae* bacterium EhC02 and *Roseovarius*
293 *indicus* EhC03, as well as *Sphingomonadales* bacterium EhC05, all isolated from *E. huxleyi*

9

294   cultures (63) (Fig. 3d). This was also evident in the genomes of several *Marinobacter*s, a genus

295   known to be associated with *E. huxleyi* cultures (63–65). *Ruegeria pomeroyi* DSS-3 was the only

296   bacterial strain included in our analysis, which is not directly associated to *E. huxleyi* but showed

297   benzoate utilization, consistent with previous observations (30). This suggests that benzoate

298   produced by *E. huxleyi* can mediate interactions of the alga with other bacteria that consume and

299   benefit from this metabolite.

300   We next examined the impact of benzoate on the lifestyle of *Sulfitobacter* D7 during

301   interactions with *E. huxleyi*. We followed the dynamics of a co-culture of *Sulfitobacter* D7 and *E.*

302   *huxleyi* (strain CCMP2090) in which the bacterial lifestyle switch, from coexistence to pathogenic,

303   does not naturally occur (Fig. 5a-b). This is attributed to the low concentrations of DMSP in the

304   media of this specific *E. huxleyi* strain (13). Indeed, bacterial pathogenicity was induced only when

305   we added external DMSP, leading to the decline of *E. huxleyi* abundance (Fig. 5b). These results

306   are consistent with our previous findings (13). When we added benzoate we did not observe any

307   change in the dynamics of algal growth, but bacterial growth was enhanced by 10-fold at day 3,

308   compared to the non-supplemented and DMSP-supplemented co-cultures (Fig. 5c). This goes

309   along with the observation of benzoate being a remarkable metabolite for *Sulfitobacter* D7 growth

310   (Fig. 4C). When we applied both benzoate and DMSP, bacterial growth was enhanced and algal

311   growth was not compromised although *Sulfitobacter* D7 and DMSP were present in high

312   concentrations. Intriguingly, the presence of benzoate negated the pathogenicity-inducing effect of

313   DMSP on *Sulfitobacter* D7. Moreover, bacterial abundance in both benzoate-added treatments was

314   higher than in the pathogenicity-inducing DMSP treatment, which demonstrates that the onset of

315   pathogenicity is decoupled from bacterial density. This suggests that benzoate is important to

316   maintain *E. huxleyi*-*Sulfitobacter* D7 coexistence and prevents the onset of bacterial pathogenicity.

317   This observation strengthens our previous conclusion that DMSP signaling in *Sulfitobacter* D7

318   depends on additional algae-derived metabolites which affect the bacterial lifestyle switch during

319   interactions with *E. huxleyi*.

320

Discussion

321

Signaling role of DMSP and other algal infochemicals in the lifestyle switch of *Sulfitobacter*

322

D7

323

324   In this study, we aimed to unravel the molecular basis for the lifestyle switch from

325   coexistence to pathogenicity in *Sulfitobacter* D7 during interactions with the bloom-forming algae

326   *E. huxleyi*. We substantiated the signaling role of algal DMSP that mediates the shift towards

327   pathogenicity by mapping the transcriptional profiles of *Sulfitobacter* D7 in response to DMSP and

10

328   other algal infochemicals. However, DMSP signaling in media that lacked *E. huxleyi*-derived

329   metabolites (i.e., MM±DMSP) had a different effect on *Sulfitobacter* D7 transcriptome. We propose

330   that the signaling role of DMSP that mediates the coexistence to pathogenicity lifestyle switch in

331   *Sulfitobacter* D7 depends on other infochemicals produced by *E. huxleyi*. DMSP is a ubiquitous

332   infochemical produced by many phytoplankton species as well as some bacteria (66), making it a

333   prevalent signaling molecule that mediates microbial interactions in the marine environment.

334   Therefore it is likely that other algal metabolites are involved in the recognition of the specific

335   phytoplankter host by bacteria, thus ensuring specificity in DMSP signaling during interactions. In

336   complex environments, where many microbial species are present simultaneously, such a

337   mechanism can ensure that bacteria will invest in altering gene expression and metabolic

338   remodeling only when the right algal partners are present.

339   We revealed that the alga-derived aromatic compound benzoate plays a pivotal role in

340   *Sulfitobacter* D7-*E. huxleyi* interaction by maintaining the coexistence, even when DMSP was

341   present at high concentrations (Fig. 5). Benzoate also acts as an efficient bacterial growth factor

342   serving as a carbon source. These observations provide a possible explanation for the switch in

343   bacterial behavior from coexistence to pathogenicity. During the interaction, *E. huxleyi* provides

344   benzoate and other growth substrates to *Sulfitobacter* D7, which uptakes and consumes them (Fig.

345   6). We propose that as long as *Sulfitobacter* D7 benefits from the interaction with *E. huxleyi* by

346   receiving beneficial growth substrates it will maintain in a coexisting lifestyle. When the growth

347   substrates provided by the alga are less beneficial, the opportunistic pathogen will switch to killing

348   the algal host, which will in turn lead to a surge of intracellular *E. huxleyi*-derived metabolites that

349   *Sulfitobacter* D7 can benefit from (Fig. 6). Studies on phytoplankton exudation of organic matter

350   demonstrated that algae release more organic matter in stationary growth, but the chemical

351   composition is different than that of exponential growth (67, 68). In nutrient limiting conditions,

352   which often occurs in stationary phase, the organic matter exuded by phytoplankton is less

353   favorable for bacterial uptake and consumption for growth (69). In such a chemical context, high

354   concentrations of algae-derived infochemicals, e.g. DMSP, can be perceived by bacteria and signal

355   that the physiological state of the algal host is deteriorating. Namely, by sensing the change in the

356   metabolic composition *Sulfitobacter* D7 executes its pathogenicity against a compromised *E.*

357   *huxleyi* population. Therefore, the initial coexistence phase is a prerequisite for the onset of

358   bacterial pathogenicity.

359   The ability to utilize benzoate is shared among bacterial strains that are associated with *E.*

360   *huxleyi* in the natural environment and in cultures (Fig. 4d) (28, 63–65). Since benzoate can act

361   as an antibacterial compound (70, 71), we propose that secretion of benzoate by *E. huxleyi* can

362   select for bacteria that specialize on this compound and is therefore important for the establishment

11

363   of a coexistence phase. Similarly, the diatom *Asterionellopsis glacialis* produces two unique

364   secondary metabolites, that selects for specific bacteria and also affect their behavioral response

365   (72). Bacterial sensing of general phytoplankton-derived compounds (e.g. DMSP) together with

366   more specific compounds (e.g. benzoate) can ensure the recognition of the algal host by the

367   bacteria within the phycosphere. This can increase the specificity of an interaction and ensure fine-

368   tuning of the behavior of the microorganisms by regulating gene expression. Molecular

369   mechanisms in bacteria that integrate information perceived by various chemical signals include

370   catabolite repression and two-component systems, which can also play a role in regulating bacterial

371   pathogenicity (73, 74).

The lifestyle switch of *Sulfitobacter* D7 from coexistence to pathogenicity

373   The experimental setup in our study demonstrated that *Sulfitobacter* D7 grown in

374   pathogenicity-inducing media are in a different transcriptional state than in coexistence medium,

375   which corresponds to the behavioral shift during co-culturing with *E. huxleyi* (Fig. 1). Many transport

376   systems were differentially expressed, mainly upregulated, when *Sulfitobacter* D7 was in

377   pathogenic state compared to the coexistence state (Fig. 3). Since bacteria often exert their

378   pathogenicity as a mean to access nutrients released from the host, it is likely that in this mode

379   *Sulfitobacter* D7 will maximize uptake and assimilation of metabolites released by dying *E. huxleyi*

380   cells. High expression of transporters for branched-chain amino acids, C4 carbohydrates, DMSP,

381   taurine and spermidine/putrescine, can facilitate the efficient uptake of these energy-rich

382   metabolites (Fig. 3, Table S6). Upregulation of transport genes for these metabolic currencies in

383   response to DMSP was also demonstrated in *R. pomeroyi* DSS-3, a Roseobacter often used to

384   study bacterial metabolic exchange with phytoplankton (5, 35, 37).

385   During the pathogenic lifestyle there was upregulation of flagellar genes, which was

386   functionally validated by the motility assay (Fig. 2). While DMSP is a known chemoattractant and

387   therefore mediates the establishment of bacterial interactions with algae (33, 36), we speculate that

388   this is not the case for *Sulfitobacter* D7 since its genome does not encode for known chemotaxis

389   genes. We propose that the increased motility in response to DMSP in the pathogenic mode can

390   serve as an ecological strategy to avoid competition with other bacteria in the phycosphere (75).

391   *E. huxleyi* cell death, induced by *Sulfitobacter* D7, likely leads to a surge of intracellular metabolites

392   that may attract other bacteria. The upregulation of flagellar motility together with transport systems

393   can enable efficient substrate uptake by *Sulfitobacter* D7 and swimming away to forage for

394   alternative metabolically active hosts. Such an "eat-and-run" strategy can be ecologically beneficial

395   by facilitating the evasion from competition.

396   Upregulation of flagellar genes was also demonstrated during the mutualistic to pathogenic

397   lifestyle switch of the Roseobacter *Dinoroseobacter shibae* during interactions with a dinoflagellate

398   algal host (76). Even though *Sulfitobacter* D7 motility was increased in pathogenic mode (Fig. 2),

399   the involvement of the flagellum may be by its alternative functions that mediate bacterial virulence

400   (77); i.e., flagella can mediate biofilm formation and attachment to surfaces (19). Additionally, the

401   flagellar type 3 secretion system (T3SS), which is found in the basal body and necessary for

402   secretion of the components needed for flagellum assembly, can also be used as an export system

403   for effector proteins in pathogenic bacteria (78). In this manner pathogenic bacteria can utilize the

404   flagellum for multiple functions important for pathogenicity against their hosts and subsequent

405   dispersal.

406   **Ecological context of bacterial lifestyle switches during algal blooms**

407   Bacterial lifestyle switches are evident in several model systems of phytoplankton-bacteria

408   interactions, however the ecological significance of such modes of interactions in the natural

409   environment is elusive. In this study, we provide a contextual framework for the switch from

410   coexistence to pathogenicity – metabolite exhaustion in the phycosphere. During a phytoplankton

411   bloom heterotrophic bacteria can support the growth of the algae and benefit from organic matter

412   released to the phycosphere. As the bloom progresses, various factors, such as nutrient depletion,

413   viral infection and grazing, can compromise the algal population and its ability to provide essential

414   metabolic currencies for optimal bacterial growth. We propose that bacteria can sense the host

415   physiological state, by infochemicals secreted from stressed algae, and switch their behavior to

416   pathogenic. This will result in algal cell death and bacterial proliferation, which could eventually

417   contribute to the bloom demise. Therefore, phytoplankton-associated opportunistic bacterial

418   pathogens constitute an underappreciated component in the regulation of algal blooms dynamics.

419   Investigating the dynamic microscale interactions of such bacteria with phytoplankton and the

420   metabolic crosstalk that mediate them, can provide insights into their impact on large scale

421   biogeochemical processes in the marine environment.

422

423   **Materials and Methods**

424   ***E. huxleyi* cultures maintenance and co-culturing with *Sulfitobacter* D7**

425   *E. huxleyi* strains were purchased from the National Center for Marine Algae (NCMA) and

426   maintained in filtered sea water (FSW). CCMP379, were cultured in f/2 medium (-Si) (79) and

427   CCMP2090 was cultured in k/2 medium (-Tris, -Si) (80). Cultures were incubated at 18°C with a

428   16:8 h, light:dark illumination cycle. A light intensity of 100 µmol photons m^{-2} s^{-1} was provided by

429   cool white LED lights. For all co-culturing experiments *E. huxleyi* cultures were inoculated at early

430 exponential growth phase ($4-8·10^5$ cell mL^{-1}) with 10^3 mL^{-1} *Sulfitobacter* D7 at t = 0d. When noted,

431 DMSP or benzoate were added at t = 0d at final concentration of 100 µM.

432

Enumeration of algae and bacteria abundances by flow cytometry

434 Flow cytometry analyses were performed on Eclipse iCyt flowcytometer (Sony Biotechnology Inc.,

435 Champaign, IL, USA) equipped with 405 and 488 nm solid-state air-cooled lasers, and with

436 standard optic filter set-up. *E. huxleyi* cells were identified by plotting the chlorophyll fluorescence

437 (663–737 nm) against side scatter and were quantified by counting the high-chlorophyll events. For

438 bacterial counts, samples were fixed with a final concentration of 0.5% glutaraldehyde for at least

439 30 min at 4°C, then plunged into liquid nitrogen and stored at −80°C until analysis. After thawing,

440 samples were stained with SYBR gold (Invitrogen) that was diluted 1:10,000 in Tris–EDTA buffer,

441 incubated for 20 min at 80°C and cooled to room temperature. Samples were analyzed by flow

442 cytometry (ex: 488 nm; em: 500–550 nm).

443

Bacterial growth media

445 The conditioned media, Exp-CM and Stat-CM, were obtained from exponential and stationary *E.*

446 *huxleyi* CCMP379 mono-cultures (Table S1), respectively, by gentle gravity filtration on GF/C filters.

447 This method was chosen to prevent lysis of algal cells during the procedure and thus ensuring that

448 only extracellular algae-derived metabolites, infochemicals and other components will reside in the

449 media. CM were subsequently filtered through 0.22 µm. Exp-CM and Stat-CM were harvested on

450 the same day of the experiment. When indicated, 100 µM DMSP was added to Exp-CM, herein

451 Exp-CM+DMSP. MM was based on artificial sea water (ASW) (81) supplemented with basal

452 medium (-Tris) (BM, containing essential nutrients) (82), vitamin mix (83), 0.5 mM NaNO3 and

453 metal mix of k/2 medium (80). For the transcriptome experiment, MM were supplemented with 1 gr

454 L^{-1} glycerol. When indicated, 100 µM DMSP was added to MM, herein MM+DMSP. For the

455 experiment presented in Fig. 4c, 100 µM benzoate were added as sole carbon source.

456

Bacterial inoculation into growth media and *E. huxleyi* cultures

458 Bacteria were inoculated into marine broth (Difco 2216) from a glycerol stock (kept at -80°C) and

459 grown over-night at 28°C, 160 rpm. Bacteria were washed three times in FSW or ASW by

460 centrifugation (10,000 g, 1 min). Bacterial inocula were counted by flow cytometry and 10^4 bacteria

461 mL^{-1} were inoculated to CM or MM, and 10^3 bacteria mL^{-1} were inoculated to *E. huxleyi* cultures.

462   *Sulfitobacter* **D7 Transcriptome**

463   *Library preparation and sequencing*

464   Experimental setup is elaborated in Fig. 1b. Samples for bacterial growth and RNA were taken at t

465   = 24h. Bacterial cell pellets were obtained from 200 mL (MM treatments) or 160 mL (CM treatments)

466   cultures by 2-step centrifugation: 10,000g, 10 min followed by 14,000g, 10 min, all at 4°C. Pellets

467   were flash frozen in liquid nitrogen and stored at -80°C until further analysis. RNA extraction was

468   carried out using the RNeasy Plant Mini Kit (Qiagen, Hilden, Germany). For disruption of cell pellets

469   we used the OmniLyse lysis kit (Claremontbio). The rest of the RNA extraction protocol was

470   according to manufacturer's instruction. Library preparation was carried out according to the RNA-

471   seq protocol developed by Avraham *et al.,* (50). Briefly, DNA was removed using TURBO DNase

472   (Ambion), RNA was fragmented and phosphorylated (at the 3'prime) using FastAP thermosensitive

473   alkaline phosphatase (Thermo Scientific). RNA from each sample was ligated with unique RNA

474   barcoded adaptors at the 3', ensuring the strandedness of each transcript, using T4 RNA ligase 1

475   (NEB). RNA samples were pooled and treated with RiboZero (Gram-Negative Bacteria) kit

476   (Illumina, San Diego, CA, USA) following manufacturer's instructions in order to remove ribosomal

477   RNA. Samples were reversed transcribed using AffinityScript RT Enzyme (Agilent) to form cDNA,

478   and amplified by PCR. The libraries were sequenced at the Weizmann Institute of Science Core

479   Facilities on an Illumina NextSeq500 high output v2 kit (paired end, 150 cycles).

480   *Transcriptome analysis*

481   Raw reads (64.5 million) were quality trimmed using Cutadapt (84) (-q 20 -m 20) in addition to

482   removal of adapters. Reads were mapped to *Sulfitobacter* D7 genome assembly

483   (GCA_003611275.1) using Bowtie2 (85) in end-to-end mode, and reads were counted on genes

484   using HTseq, in the strict mode (86). Final reads per sample can be found in Table S12. Gene

485   expression was quantified using DESeq2 (87) (Table S2). Differentially expressed genes were

486   selected as genes with adjusted *P*-value <0.05, and |fold change|>2, and basemean >10 (the

487   average of the normalized count values, dividing by size factors, taken over all samples). Priciple

488   component analysis and similarity between samples were calculated using DESeq2 and visualized

489   using RStudio 3.5.0. Heatmaps of gene expression were calculated using the log-normalized

490   expression values (rld), with row standardization (scaling the means of a row to zero, with standard

491   deviation of 1), and visualized using Partek Genomics Suite 7.0 software, Heatmapper (88) and

492   Excel. The data has been deposited in NCBI's Gene Expression Omnibus (GEO) and is available

493   through GEO series accession number GSE193203.

494

495   **Functional enrichment in KEGG Pathways**

496   Differentially expressed genes in the comparisons Exp-CM+DMSP vs. Exp-CM, Stat-CM vs. Exp-

497   CM and MM+DMSP vs. MM were clustered using k-means analysis. For each cluster, enriched

498 KEGG pathways (with Padj <0.01) were calculated by g:Profiler (89), using a customized reference

499 which was constructed from *Sulfitobacter* D7 specific KEGG pathways.

500

501 **_Sulfitobacter_ D7 genome mining and manual annotation**

502 The automatic NCBI Prokaryotic Genome Annotation Pipeline was used for *Sulfitobacter* D7

503 genome functions prediction (43). We manually validated the function of genes related to DMSP

504 metabolism, transport, benzoate degradation and flagella assembly by cross examining their

505 annotation using KEGG, COG and IMG/M. For genes with no or inconsistent annotation, we also

506 searched for functional domains using the Conserved Domain Database (CDD), and we ran BLAST

507 using genes with known functions to validate the annotation.

508 *Transport genes*

509 The automatic annotations of transport genes were manually validated by ensuring that the genes

510 were annotated as such by at least two automatic annotation platforms and by CDD search. Since

511 transport systems are organized in operon-like structures, we examined the genes adjacent to the

512 transport genes and manually annotated these additional transport genes. The transporters

513 presented in the heatmap (Fig. 3) are the full transport systems that at least two of the genes in

514 each system were DE. The Venn diagrams (Fig. S2) contains only the transport genes that were

515 significantly DE. The substrates for each transport system were inferred automatically, therefore,

516 the exact substrates were not experimentally validated.

517 *Benzoate degradation genes*

518 *Sulfitobacter* D7 benzoate degradation pathway was reconstructed using the KEGG mapping tool

519 (90). All the genes in the catechol branch of benzoate degradation (Fig. S3) were found, except

520 Muconolactone isomerase *CatC*. For the visualization of the organization of the genetic locus of

521 benzoate-related genes we utilized the IMG/M platform (91).

522 *Flagellar genes*

523 We manually validated the annotation of all the flagella genes in *Sulfitobacter* D7 genome and

524 found most of the genes, except for three: *FliQ*, *FliJ* and *FliD* (92). For the visualization of the

525 organization of the genetic locus of flagellar genes we utilized the IMG/M platform (91).

526

527 **Bacterial motility assay**

528 Motility was assessed by examining the expansion of bacterial colonies plated on semi-solid agar

529 (93). Semi-solid media of Exp-CM, Exp-CM+DMSP and Stat-CM were prepared by mixing boiling

530 sterile 3% agarose with CM, which was pre-heated to ~50°C, in a 1:9 ratio (final concentration of

531 0.3% agarose). Media was quickly distributed in 6-well plates, ~5 mL per plate, and was left to

532   solidify for ~ 1 h. *Sulfitobacter* D7 were pre-grown in liquid Exp-CM, Exp-CM+DMSP and Stat-CM

533   in order to induce the appropriate expression of flagellar genes. For control, bacteria were pre-

534   grown in liquid ½MB, lacking algal DMSP and infochemicals. After 24 h bacterial abundance was

535   evaluated and the concentration of bacteria in each media was normalized to $2 \cdot 10^6$ mL^{-1}, to ensure

536   that the difference in colony size would be indicative of motility and not abundance of bacteria.

537   Bacteria grown in CM were plated on the corresponding semi-solid CM (0.3% agarose) and

538   bacteria grown in ½MB were plated on each semi-solid CM. For plating, 1 μL of bacteria were

539   pipetted in the center of each well containing semi-solid media, in 10-12 replicates per treatment.

540   Colonies were visualized with 2X magnification after 6 days using Nikon SMZ18 Steriomicroscope.

541   Colonies measurements were performed using the Annotation and Measurements tool of the Nikon

542   NIS-Elements Analysis D software.

543

544   **Quantification of benzoate in media extracts**

545   To quantify extracellular benzoate concentrations, cultures were filtered gently over 0.22 μm filters,

546   acidified, and led through hydrophilic-lipophilic balanced solid phase extraction (SPE) cartridges,

547   as described in Kuhlisch et al. (94). Glassware and chemically resistant equipment were used

548   whenever possible and cleaned with HCl (1% or 10%) and Deconex 20 NS-x (Borer Chemie,

549   Zuchwil, Switzerland) to reduce contaminations. Per sample, 50 mL (bacterial cultures) or 300 mL

550   (algal cultures) of filtrate was collected in glass Erlenmeyer flasks and spiked with 5 μL of benzoate-

551   d$_5$ (98%, Cambridge Isotope Laboratries, Tewsbury, MA, USA; 1.276 μg/μL in MeOH) for 1 μM final

552   concentration, as internal standard. The filtrates were incubated for 30 min and then acidified to pH

553   2.0 using 10% HCl. Metabolites were extracted using hydrophilic-lipophilic balanced SPE

554   cartridges (Oasis HLB, 200 mg, Waters, Milford, MA, USA) as follows: cartridges were conditioned

555   (6 mL methanol), equilibrated (6 mL 0.01 N HCl), and then loaded by gravity with the acidified

556   samples (45 min). The cartridges were then washed (18 mL 0.01 N HCl), dried completely using a

557   vacuum pump, and gravity-eluted with 2× 2 mL methanol into 4 mL glass vials. Eluates were stored

558   at -20°C, dried under a flow of nitrogen at 0.5 mL/min and 30°C (TurboVap LV, Biotage, Uppsala,

559   Sweden), and stored at -20°C until further processing. Dried extracts were thawed, re-dissolved in

560   300 μL methanol:water (1:1, v:v), vortexed, sonicated for 10 min, and centrifuged at 3,200×g for 10

561   min at 4°C. The supernatants were transferred to 200 μL glass inserts in autosampler vials and

562   analyzed by ultra-high-performance liquid chromatography-electrospray-high resolution mass

563   spectrometry (UHPLC-ESI-HRMS). An aliquot of 1 μL was analyzed using UPLC coupled to a

564   photodiode detector (ACQUITY UPLC I-Class, Waters) and a quadrupole time-of-flight (QToF)

565   mass spectrometer (SYNAPT G2 HDMS, Waters), as described previously with slight

566   modifications. Chromatographic separation was carried out using an ACQUITY UPLC BEH C18

567   column (100 × 2.1 mm, 1.7 μm; Waters) attached to a VanGuard pre-column (5 × 2.1 mm, 1.7 μm;

568   Waters). The mobile phase, at a flow rate of 0.3 mL/min, consisted of water (mobile phase A) and

569   acetonitrile (mobile phase B), both with 0.1% formic acid, and set as follows: a liner gradient from

570   100-75% A in 20 min, from 75-0% A in 6 min, 2 min of 100% B, and 2 min to return to the initial

571   conditions and re-equilibrate the column. The PDA detector was set to 200-600 nm. A divert valve

572   (Rheodyne) excluded 0-1 min and 25.5-30 min from injection to the mass spectrometer. The ESI

573   source was operated in negative ionization mode and set to 140°C source and 450°C desolvation

574   temperature, 1.0 kV capillary voltage, and 27 eV cone voltage, using nitrogen as desolvation gas

575   (800 L/h) and cone gas (10 L/h). The mass spectrometer was operated in full scan MSE resolution

576   mode with a mass range of 50-1600 Da and the mass resolution tuned to 23,000 at m/z 554

577   alternating with 0.1 min scan time between low- (4 eV collision energy) and high-energy scan

578   function (collision energy ramp of 15-50 eV).

579   An external calibration curve was processed in parallel. Aliquots of 100 mL artificial seawater

580   (ASW) were spiked with 10 µL of d5-benzoate as internal standard (IS) (1 µM final concentration)

581   and benzoate standard solutions to reach final concentrations of 0.2, 1, 2, 10, 20, and 100 µM

582   benzoate. Two blanks were prepared, one blank that was spiked only with the IS, and one blank

583   lacking both IS and benzoate. Each sample was divided to duplicates of 50 mL and extracted as

584   described above. After re-dissolving in 200 µL methanol:water (1:1, v:v), samples were injected

585   subsequent to the biological samples. The peak areas of the [M-H]$^-$ ions for the IS (*m*/*z* 126.06)

586   and benzoate (*m*/*z* 121.029) were extracted above a signal-to-noise threshold of 10 using

587   QuanLynx (Version 4.1, Waters), and the analyte response calculated by dividing the area of

588   benzoate by the IS (Fig. S5). The response (y) was then plotted against the concentration of

589   benzoate (x), and the slope and intercept for a linear regression calculated (y = 0.4741x + 1.665,

590   R^2 = 0.99) (Fig. S5). Quantification of the samples was done based on the analyte response in

591   each sample and the calibration curve. The limit of quantification was 200 nM.

592

593   **Prevalence of benzoate transport and catabolism genes in genomes of phytoplankton-**

594   **associated bacteria**

595   Bacterial benzoate degradation pathways and the genes encoding for the metabolic enzymes were

596   reconstructed with the use of MetaCyc (95) and the KEGG Pathway database (96) (Fig. S3).

597   Selected genes, encoding for benzoate transporters and for the enzymes mediating the initial steps

598   of benzoate metabolism in each pathway, were used to search for similar proteins in bacterial

599   genomes using BLASTp. The list of these query genes, which were all previously experimentally

600   validated, is found in Table S10. The target bacterial genomes were selected based on their known

601   association with *E. huxleyi* and other phytoplankton species (Table S9). Positive hits had an E-

602   value <0.005, identity > 30% and coverage >30. Hits with lower coverage and/or identity were

603   considered as "Partial". The results are summarized in Table S9.

604 **Statistical analyses**

605 For the motility assay (Fig. 2b) we used 2-way ANOVA, followed by Tukey's post-hoc test, using

606 the R-package "emmeans". For benzoate consumption (Fig. 4c) we used a mixed effects model,

607 with treatment and time as fixed effects, and replicate as a random effect, using the R package's

608 "lme4" and "lmerTest". For the *E. huxleyi* growth curves (Fig. 5 a,b) we used a mixed effects model,

609 with treatment, bacteria (none or D7) and time as fixed effects, and replicate as a random effect.

610 For the bacterial growth curves (Fig. 5c) we used a mixed effects model, with treatment and time

611 as fixed effects, and replicate as a random effect. Slopes within the mixed models were compared

612 using the 'emmeans' package. *P*-values for all comparisons are presented in Table S11. All

613 analyses were done using R, v. 4.1.2.

614

615 **Figures preparation**

616 Figures and illustrations were prepared using PowerPoint, Excel and BioRender.com.

617

618 # Acknowledgments

624

625 # References

626 1.   C. B. Field, M. J. Behrenfeld, J. T. Randerson, P. Falkowski, Primary Production of the
627   Biosphere: Integrating Terrestrial and Oceanic Components. *Science* **281**, 237–240 (1998).

628 2.   J. R. Seymour, S. A. Amin, J.-B. Raina, R. Stocker, Zooming in on the phycosphere: the
629   ecological interface for phytoplankton–bacteria relationships. *Nat. Microbiol.* **2**, 17065
630   (2017).

631 3.   E. Cirri, G. Pohnert, Algae−bacteria interactions that balance the planktonic microbiome.
632   *New Phytol.* **223**, 100–106 (2019).

633 4.   W. Bell, R. Mitchell, Chemotactic and growth responses of marine bacteria to algal
634   extracellular products. *Biol. Bull.* **143**, 265–277 (1972).

635 5.   M. Landa, A. S. Burns, S. J. Roth, M. A. Moran, Bacterial transcriptome remodeling during
636   sequential co-culture with a marine dinoflagellate and diatom. *ISME J.* **11**, 2677–2690
637   (2017).

638 6.   E. Segev, *et al.*, Dynamic metabolic exchange governs a marine algal-bacterial interaction.
639   *Elife* **5**, e17473 (2016).

640 7.   H. Wang, J. Tomasch, M. Jarek, I. Wagner-Döbler, A dual-species co-cultivation system to

641   study the interactions between *Roseobacters* and dinoflagellates. *Front. Microbiol.* **5**, 311
642   (2014).

643   8.   S. A. Amin, *et al.*, Photolysis of iron-siderophore chelates promotes bacterial-algal
644   mutualism. *Proc. Natl. Acad. Sci.* **106**, 17071–17076 (2009).

645   9.   M. T. Croft, A. D. Lawrence, E. Raux-Deery, M. J. Warren, A. G. Smith, Algae acquire
646   vitamin B_{12} through a symbiotic relationship with bacteria. *Nature* **438**, 90–93 (2005).

647   10. G. Pohnert, M. Steinke, R. Tollrian, Chemical cues, defence metabolites and the shaping of
648   pelagic interspecific interactions. *Trends Ecol. Evol.* **22**, 198–204 (2007).

649   11. M. R. Seyedsayamdost, R. J. Case, R. Kolter, J. Clardy, The Jekyll-and-Hyde chemistry of
650   *Phaeobacter gallaeciensis*. *Nat. Chem.* **3**, 331–335 (2011).

651   12. S. A. Amin, *et al.*, Interaction and signalling between a cosmopolitan phytoplankton and
652   associated bacteria. *Nature* **522**, 98–101 (2015).

653   13. N. Barak-Gavish, *et al.*, Bacterial virulence against an oceanic bloom-forming phytoplankter
654   is mediated by algal DMSP. *Sci. Adv.* **4**, eaau5716 (2018).

655   14. R. N. Slightom, A. Buchan, Surface Colonization by Marine Roseobacters: Integrating
656   Genotype and Phenotype. *Appl. Environ. Microbiol.* **75**, 6027–6037 (2009).

657   15. R. Stocker, J. R. Seymour, Ecology and physics of bacterial chemotaxis in the ocean.
658   *Microbiol. Mol. Biol. Rev.* **76**, 792–812 (2012).

659   16. G. Furusawa, T. Yoshikawa, A. Yasuda, T. Sakata, Algicidal activity and gliding motility of
660   *Saprospira* sp. SS98-5. *Can. J. Microbiol.* **49**, 92–100 (2003).

661   17. T. R. Miller, R. Belas, Motility is involved in *Silicibacter* sp. TM1040 interaction with
662   dinoflagellates. *Environ. Microbiol.* **8**, 1648–1659 (2006).

663   18. E. C. Sonnenschein, D. A. Syit, H.-P. Grossart, M. S. Ullrich, Chemotaxis of *Marinobacter*
664   *adhaerens* and its impact on attachment to the diatom *Thalassiosira weissflogii*. *Appl.*
665   *Environ. Microbiol.* **78**, 6900–7 (2012).

666   19. Y. Li, *et al.*, Chitinase producing bacteria with direct algicidal activity on marine diatoms. 1–
667   13 (2016).

668   20. C. Fei, *et al.*, Quorum sensing regulates 'swim-or-stick' lifestyle in the phycosphere. *Environ.*
669   *Microbiol.* **22**, 4761–4778 (2020).

670   21. X. Mayali, P. J. S. Franks, F. Azam, Cultivation and ecosystem role of a marine *Roseobacter*
671   clade-affiliated cluster bacterium. *Appl. Environ. Microbiol.* **74**, 2595–2603 (2008).

672   22. A. Buchan, G. R. LeCleir, C. A. Gulvik, J. M. González, Master recyclers: features and
673   functions of bacteria associated with phytoplankton blooms. *Nat. Rev. Microbiol.* **12**, 686–
674   698 (2014).

675   23. B. Rink, *et al.*, Effects of phytoplankton bloom in a coastal ecosystem on the composition of
676   bacterial communities. *Aquat. Microb. Ecol.* **48**, 47–60 (2007).

677   24. J. M. González, M. A. Moran, Numerical dominance of a group of marine bacteria in the
678   alpha-subclass of the class Proteobacteria in coastal seawater. *Appl. Environ. Microbiol.*
679   **63**, 4237–4242 (1997).

680   25. M. Alavi, T. Miller, K. Erlandson, R. Schneider, R. Belas, Bacterial community associated
681   with *Pfiesteria*-like dinoflagellate cultures. *Environ. Microbiol.* **3**, 380–396 (2001).

682   26. S. A. Amin, M. S. Parker, E. V. Armbrust, Interactions between diatoms and bacteria.

20

683   *Microbiol. Mol. Biol. Rev.* **76**, 667–684 (2012).

684   27.   G. Behringer, *et al.*, Bacterial communities of diatoms display strong conservation across
685   strains and time. *Front. Microbiol.* **9**, 1–15 (2018).

686   28.   F. Vincent, *et al.*, Viral infection switches the balance between bacterial and eukaryotic
687   recyclers of organic matter during algal blooms. *bioRxiv*, 2021.10.25.465659 (2021).

688   29.   H. Geng, R. Belas, Molecular mechanisms underlying roseobacter-phytoplankton
689   symbioses. *Curr. Opin. Biotechnol.* **21**, 332–8 (2010).

690   30.   R. J. Newton, *et al.*, Genome characteristics of a generalist marine bacterial lineage. *ISME
691   J.* **4**, 784–798 (2010).

692   31.   M. D. Keller, Dimethyl Sulfide Production and Marine Phytoplankton: The Importance of
693   Species Composition and Cell Size. *Biol. Oceanogr.* **6**, 375–382 (1989).

694   32.   T. R. Miller, R. Belas, Dimethylsulfoniopropionate metabolism by *Pfiesteria*-associated
695   *Roseobacter* spp. *Appl. Environ. Microbiol.* **70**, 3383–3391 (2004).

696   33.   T. R. Miller, K. Hnilicka, A. Dziedzic, P. Desplats, R. Belas, Chemotaxis of *Silicibacter* sp.
697   strain TM1040 toward dinoflagellate products. *Appl. Environ. Microbiol.* **70**, 4692–4701
698   (2004).

699   34.   P. Sule, R. Belas, A novel inducer of Roseobacter motility is also a disruptor of algal
700   symbiosis. *J. Bacteriol.* **195**, 637–46 (2013).

701   35.   H. Bürgmann, *et al.*, Transcriptional response of *Silicibacter pomeroyi* DSS-3 to
702   dimethylsulfoniopropionate (DMSP). *Environ. Microbiol.* **9**, 2742–2755 (2007).

703   36.   J. R. Seymour, R. Simó, T. Ahmed, R. Stocker, Chemoattraction to
704   dimethylsulfoniopropionate throughout the marine microbial food web. *Science* **329**, 342–
705   345 (2010).

706   37.   B. P. Durham, *et al.*, Cryptic carbon and sulfur cycling between surface ocean plankton.
707   *Proc. Natl. Acad. Sci.* **112**, 453–457 (2015).

708   38.   M. B. Cooper, *et al.*, Cross-exchange of B-vitamins underpins a mutualistic interaction
709   between *Ostreococcus tauri* and *Dinoroseobacter shibae*. *ISME J.* **13**, 334–345 (2019).

710   39.   A. R. Bramucci, *et al.*, The Bacterial Symbiont *Phaeobacter inhibens* Shapes the Life History
711   of Its Algal Host *Emiliania huxleyi*. *Front. Mar. Sci.* **5**, 188 (2018).

712   40.   T. J. Mayers, A. R. Bramucci, K. M. Yakimovich, R. J. Case, A Bacterial Pathogen
713   Displaying Temperature-Enhanced Virulence of the Microalga *Emiliania huxleyi*. *Front.
714   Microbiol.* **7**, 892 (2016).

715   41.   C. J. S. Bolch, T. A. Bejoy, D. H. Green, Bacterial Associates Modify Growth Dynamics of
716   the Dinoflagellate *Gymnodinium catenatum*. *Front. Microbiol.* **8**, 670 (2017).

717   42.   A. Shemi, *et al.*, Dimethyl sulfide mediates microbial predator–prey interactions between
718   zooplankton and algae in the ocean. *Nat. Microbiol.* **6**, 1357–1366 (2021).

719   43.   C. Ku, N. Barak-Gavish, M. Maienschein-Cline, S. J. Green, A. Vardi, Complete Genome
720   Sequence of *Sulfitobacter* sp. Strain D7, a Virulent Bacterium Isolated from an *Emiliania
721   huxleyi* Algal Bloom in the North Atlantic. *Microbiol. Resour. Announc.* **7**, e01379-18 (2018).

722   44.   N. Y. D. Ankrah, T. Lane, C. R. Budinoff, M. K. Hadden, A. Buchan, Draft Genome sequence
723   of *Sulfitobacter* sp. CB2047, a member of the *Roseobacter* clade of marine bacteria,
724   isolated from an *Emiliania huxleyi* Bloom. *Genome Announc.* **2**, e01125-14 (2014).

45. E. C. Howard, *et al.*, Bacterial taxa that limit sulfur flux from the ocean. *Science* **314**, 649–652 (2006).

46. J. D. Todd, *et al.*, Structural and regulatory genes required to make the gas dimethyl sulfide in bacteria. *Science* **315**, 666–9 (2007).

47. C. R. Reisch, *et al.*, Novel pathway for assimilation of dimethylsulphoniopropionate widespread in marine bacteria. *Nature* **473**, 208–211 (2011).

48. L. Sun, A. R. J. Curson, J. D. Todd, A. W. B. Johnston, Diversity of DMSP transport in marine bacteria, revealed by genetic analyses. *Biogeochemistry* **110**, 121–130 (2012).

49. A. R. J. Curson, J. D. Todd, M. J. Sullivan, A. W. B. Johnston, Catabolism of dimethylsulphoniopropionate: microorganisms, enzymes and genes. *Nat. Rev. Microbiol.* **9**, 849–859 (2011).

50. R. Avraham, *et al.*, A highly multiplexed and sensitive RNA-seq protocol for simultaneous analysis of host and pathogen transcriptomes. *Nat. Protoc.* **11**, 1477–1491 (2016).

51. S. D. Cook, An Historical Review of Phenylacetic Acid. *Plant Cell Physiol.* **60**, 243–254 (2019).

52. V. Thiel, *et al.*, Identification and biosynthesis of tropone derivatives and sulfur volatiles produced by bacteria of the marine Roseobacter clade. *Org. Biomol. Chem.* **8**, 234–246 (2010).

53. R. Wang, É. Gallant, M. R. Seyedsayamdost, Investigation of the genetics and biochemistry of roseobacticide production in the *Roseobacter* clade bacterium *Phaeobacter inhibens*. *MBio* **7**, e02118-15 (2016).

54. F. X. Ferrer-González, *et al.*, Resource partitioning of phytoplankton metabolites that support bacterial heterotrophy. *ISME J.* **15**, 762–773 (2021).

55. T. Obata, *et al.*, Gas-Chromatography Mass-Spectrometry (GC-MS) Based Metabolite Profiling Reveals Mannitol as a Major Storage Carbohydrate in the Coccolithophorid Alga *Emiliania huxleyi*. *Metabolites* **3**, 168–184 (2013).

56. Y. Tsuji, I. Suzuki, Y. Shiraiwa, Enzymological Evidence for the Function of a Plastid-Located Pyruvate Carboxylase in the Haptophyte alga *Emiliania huxleyi*: A Novel Pathway for the Production of C4 Compounds. *Plant Cell Physiol.* **53**, 1043–1052 (2012).

57. A. Buchan, E. L. Neidle, M. A. Moran, Diverse Organization of Genes of the β-Ketoadipate Pathway in Members of the Marine Roseobacter Lineage. *Appl. Environ. Microbiol.* **70**, 1658–1668 (2004).

58. M. A. Moran, *et al.*, Ecological genomics of marine roseobacters. *Appl. Environ. Microbiol.* **73**, 4559–4569 (2007).

59. C. S. Harwood, R. E. Parales, The β-ketoadipate pathway and the biology of self-identity. *Annu. Rev. Microbiol.* **50**, 553–590 (1996).

60. G. Fuchs, M. Boll, J. Heider, Microbial degradation of aromatic compounds — from one strategy to four. *Nat. Rev. Microbiol.* **9**, 803–816 (2011).

61. L. S. Collier, G. L. Gaines, E. L. Neidle, Regulation of Benzoate Degradation in *Acinetobacter* sp. Strain ADP1 by BenM, a LysR-Type Transcriptional Activator. *J. Bacteriol.* **180**, 2493–2501 (1998).

62. B. M. Bundy, L. S. Collier, T. R. Hoover, E. L. Neidle, Synergistic transcriptional activation by one regulatory protein in response to two metabolites. *Proc. Natl. Acad. Sci.* **99**, 7693–

22

768   7698 (2002).

769   63.   A. R. R. Rosana, *et al.*, Draft Genome Sequences of Seven Bacterial Strains Isolated from
770   a Polymicrobial Culture of Coccolith-Bearing (C-Type) *Emiliania huxleyi* M217. *Genome*
771   *Announc.* **4**, 9–10 (2016).

772   64.   D. H. Green, V. Echavarri-bravo, D. Brennan, M. C. Hart, Bacterial diversity associated with
773   the coccolithophorid algae *Emiliania huxleyi* and *Coccolithus pelagicus f. braarudii*. *Biomed*
774   *Res. Int.* **2015** (2015).

775   65.   F. D. Orata, *et al.*, Draft Genome Sequences of Four Bacterial Strains Isolated from a
776   Polymicrobial Culture of Naked (N-Type) *Emiliania huxleyi* CCMP1516. *Genome Announc.*
777   **4**, 9–10 (2016).

778   66.   A. R. J. Curson, *et al.*, Dimethylsulfoniopropionate biosynthesis in marine bacteria and
779   identification of the key gene in this process. *Nat. Microbiol.* **2**, 17009 (2017).

780   67.   A. Jensen, Excretion of organic carbon as function of nutrient stress. *Mar. Phytoplankt.*
781   *Product. Proc. Symp. Taormina, 1983*, 61–72 (1984).

782   68.   A. Barofsky, C. Vidoudez, G. Pohnert, Metabolic profiling reveals growth stage variability in
783   diatom exudates. *Limnol. Oceanogr. Methods* **7**, 382–390 (2009).

784   69.   I. Obernosterer, G. J. Herndl, Phytoplankton extracellular release and bacterial growth:
785   Dependence on the inorganic N:P ratio. *Mar. Ecol. Prog. Ser.* **116**, 247–258 (1995).

786   70.   H. Haque, T. J. Cutright, B.-M. Z. Newby, Effectiveness of sodium benzoate as a freshwater
787   low toxicity antifoulant when dispersed in solution and entrapped in silicone coatings.
788   *Biofouling* **21**, 109–119 (2005).

789   71.   D. H. Amin, A. Abolmaaty, Efficacy assessment of various natural and organic
790   antimicrobials against *Escherichia coli* O157:H7, *Salmonella enteritidis* and *Listeria*
791   *monocytogenes*. *Bull. Natl. Res. Cent.* **44**, 172 (2020).

792   72.   A. A. Shibl, *et al.*, Diatom modulation of select bacteria through use of two unique secondary
793   metabolites. *Proc. Natl. Acad. Sci.* **117**, 27445–27455 (2020).

794   73.   B. Görke, J. Stülke, Carbon catabolite repression in bacteria: many ways to make the most
795   out of nutrients. *Nat. Rev. Microbiol.* **6**, 613–624 (2008).

796   74.   D. Beier, R. Gross, Regulation of bacterial virulence by two-component systems. *Curr. Opin.*
797   *Microbiol.* **9**, 143–152 (2006).

798   75.   Y. Yawata, *et al.*, Competition-dispersal tradeoff ecologically differentiates recently
799   speciated marine bacterioplankton populations. *Proc. Natl. Acad. Sci.*, 1–6 (2014).

800   76.   H. Wang, *et al.*, Identification of Genetic Modules Mediating the Jekyll and Hyde Interaction
801   of *Dinoroseobacter shibae* with the Dinoflagellate *Prorocentrum minimum*. *Front. Microbiol.*
802   **6**, 1–8 (2015).

803   77.   B. Chaban, H. V. Hughes, M. Beeby, The flagellum in bacterial pathogens: For motility and
804   a whole lot more. *Semin. Cell Dev. Biol.* **46**, 91–103 (2015).

805   78.   A. Diepold, J. P. Armitage, Type III secretion systems: the bacterial flagellum and the
806   injectisome. *Philos. Trans. R. Soc. B Biol. Sci.* **370**, 20150020 (2015).

807   79.   R. R. L. Guillard, J. H. Ryther, Studies of marine planktonic diatoms. I. *Cyclotella nana*
808   Hustedt, and *Detonula confervacea* (cleve) Gran. *Can. J. Microbiol.* **8**, 229–239 (1962).

809   80.   M. D. Keller, R. C. Seluin, W. Claus, R. R. L. Guillard, Media for the culture of oceanic
810   ultraphytoplankton. *J. Phycol.* **23**, 633–638 (1987).

23

811   81.   C. Goyet, A. Poisson, New determination of carbonic acid dissociation constants in seawater as a function of temperature and salinity. *Deep Sea Res. Part A, Oceanogr. Res. Pap.* **36**, 1635–1654 (1989).

814   82.   P. Baumann, L. Baumann, "The marine Gram-negative eubacteria: genera *Photobacterium*, *Beneckea*, *Alteromonas*, *Pseudomonas*, and *Alcaligenes*" in *The Prokaryotes*, M. P. Starr, H. Stolp, H. G. Triiper, A. Balows, H. G. Schlegel, Eds. (Springer-Verlag, 1981), pp. 1302–1331.

818   83.   J. M. González, F. Mayer, M. A. Moran, R. E. Hodson, W. B. Whitman, *Microbulbifer hydrolyticus* gen. nov., sp. nov., and *Marinobacterium georgiense* gen. nov., sp. nov., two marine bacteria from a lignin-rich pulp mill waste enrichment community. *Int. J. Syst. Bacteriol.* **47**, 369–376 (1997).

822   84.   M. Martin, Cutadapt removes adapter sequences from high-throughput sequencing reads. *EMBnet.journal* **17**, 10 (2011).

824   85.   B. Langmead, S. L. Salzberg, Fast gapped-read alignment with Bowtie 2. *Nat. Methods* **9**, 357–359 (2012).

826   86.   S. Anders, P. T. Pyl, W. Huber, HTSeq — a Python framework to work with high-throughput sequencing data. *Bioinformatics* **31**, 166–169 (2015).

828   87.   M. I. Love, W. Huber, S. Anders, Moderated estimation of fold change and dispersion for RNA-seq data with DESeq2. *Genome Biol.* **15**, 550 (2014).

830   88.   S. Babicki, *et al.*, Heatmapper: web-enabled heat mapping for all. *Nucleic Acids Res.* **44**, W147–W153 (2016).

832   89.   U. Raudvere, *et al.*, g:Profiler: a web server for functional enrichment analysis and conversions of gene lists (2019 update). *Nucleic Acids Res.* **47**, W191–W198 (2019).

834   90.   M. Kanehisa, Y. Sato, M. Kawashima, KEGG mapping tools for uncovering hidden features in biological data. *Protein Sci.*, 1–7 (2021).

836   91.   I.-M. A. Chen, *et al.*, IMG/M: integrated genome and metagenome comparative data analysis system. *Nucleic Acids Res.* **45**, D507–D516 (2017).

838   92.   F. F. V Chevance, K. T. Hughes, Coordinating assembly of a bacterial macromolecular machine. *Nat. Rev. Microbiol.* **6**, 455–465 (2008).

840   93.   A. J. Wolfe, H. C. Berg, Migration of bacteria in semisolid agar. *Proc. Natl. Acad. Sci.* **86**, 6973–6977 (1989).

842   94.   C. Kuhlisch, *et al.*, Viral infection of algal blooms leaves a unique metabolic footprint on the dissolved organic matter in the ocean. *Sci. Adv.* **7**, 1–14 (2021).

844   95.   R. Caspi, *et al.*, The MetaCyc database of metabolic pathways and enzymes and the BioCyc collection of Pathway/Genome Databases. *Nucleic Acids Res.* **42**, D459–D471 (2014).

846   96.   M. Kanehisa, KEGG: Kyoto Encyclopedia of Genes and Genomes. *Nucleic Acids Res.* **28**, 27–30 (2000).

848   **Figures**

849
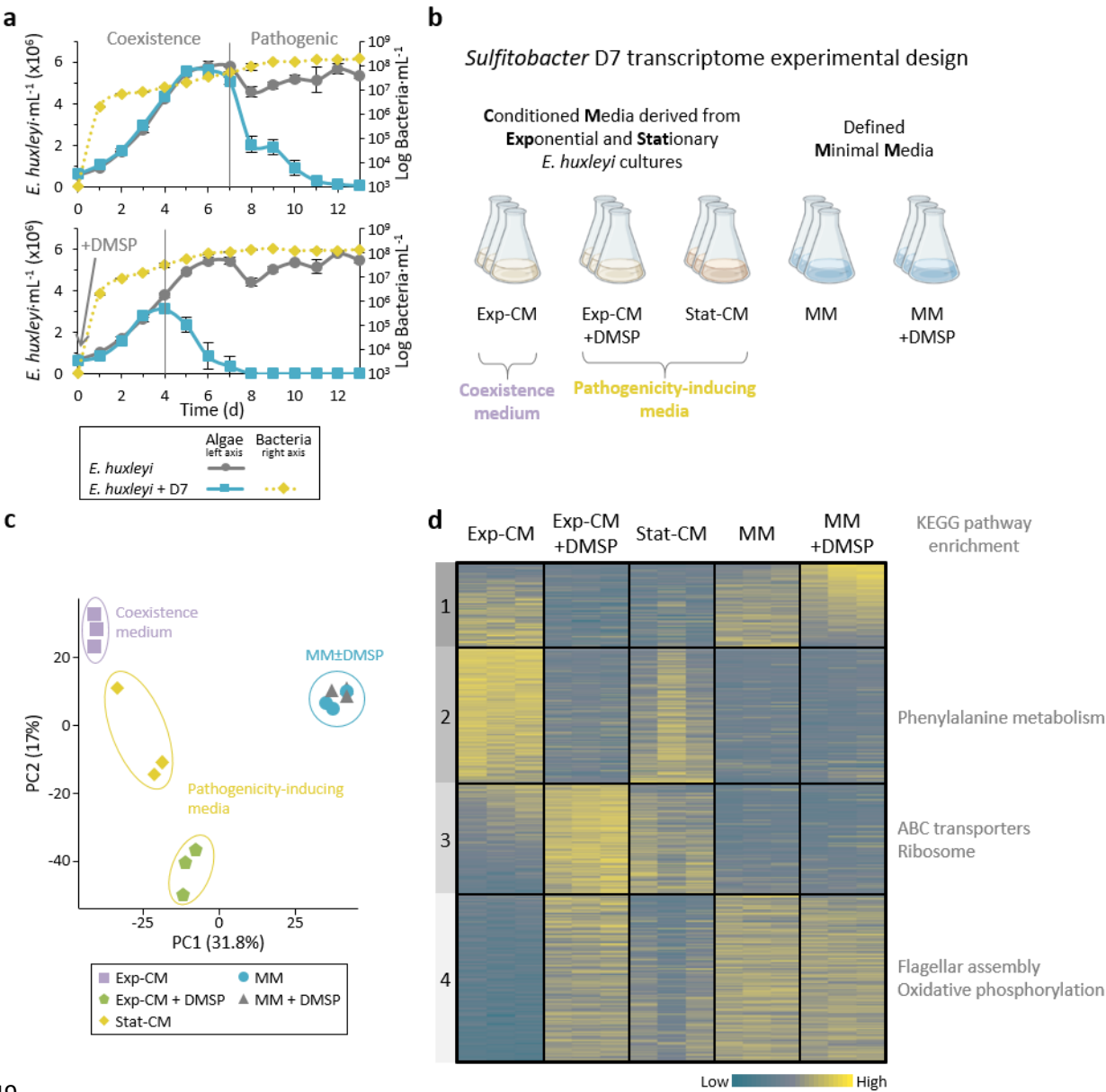
850   **Fig. 1.** **Transcriptional profiling of _Sulfitobacter_ D7 in response to DMSP and additional**
851   **_E. huxleyi_ infochemicals reveals the signaling role of DMSP.**
852   (a) Time course of _E. huxleyi_ (strain CCMP379) and bacterial abundance (full and dashed lines,
853   left and right axes, respectively) in algal mono-cultures or during co-culturing with _Sulfitobacter_ D7.
854   Top panel: Co-cultures display two phases with distinct bacterial lifestyles: coexistence and
855   pathogenicity. Bottom panel: DMSP was added at day 0 to a final concentration of 100 µM. Results
856   represent average ± SD (n = 3). Adapted from Barak-Gavish _et al._, 2018 (13) (b) Design of
857   _Sulfitobacter_ D7 transcriptome experiment aiming to explore gene expression profiles in response
858   to _E. huxleyi_-derived media and in response to DMSP. Growth media consisted of conditioned

25

859   media (CM) derived from *E. huxleyi* at exponential or stationary growth phase (Exp-CM and Stat-
860   CM, respectively), and an additional treatment in which 100 µM of DMSP was added (Exp-
861   CM+DMSP). These media differentially induce the coexistence and pathogenicity lifestyles of
862   *Sulfitobacter* D7. In order to identify DMSP-responsive genes we inoculated *Sulfitobacter* D7 in
863   defined minimal media (MM), lacking *E. huxleyi*-derived exudates, without and with 100 µM DMSP
864   (MM and MM+DMSP, respectively). *Sulfitobacter* D7 was inoculated into each media and
865   harvested for RNA profiling after 24 h of growth. Initial conditions of the media and bacterial growth
866   are elaborated in Table S1. (c) Principle component analysis of *Sulfitobacter* D7 detected genes in
867   all treatments (2588 genes). Triplicates of each treatment are shown. We observed a clear
868   separation between CM treatments and the MM treatments. (d) Heatmap of gene expression of all
869   differentially expressed (DE) genes in the comparisons Exp-CM+DMSP vs. Exp-CM, Stat-CM vs.
870   Exp-CM and MM+DMSP vs. MM (1179 genes). DE genes were defined as genes with |fold
871   change|>2 and adjusted *P*-value ≤ 0.05. Clusters were determined based on k-means analysis.
872   Significant functional enrichment in each cluster, based on KEGG Pathways, are denoted. Each
873   row represents one gene and the color intensity corresponds to the standardized expression across
874   all samples (triplicates of each treatment are shown). Expression values are scaled by row. Genes
875   in cluster 1 are ordered based on the mean expression values in the MM+DMSP treatment. Genes
876   in cluster 2-4 are ordered based on the mean expression values in the Exp-CM treatment.

877
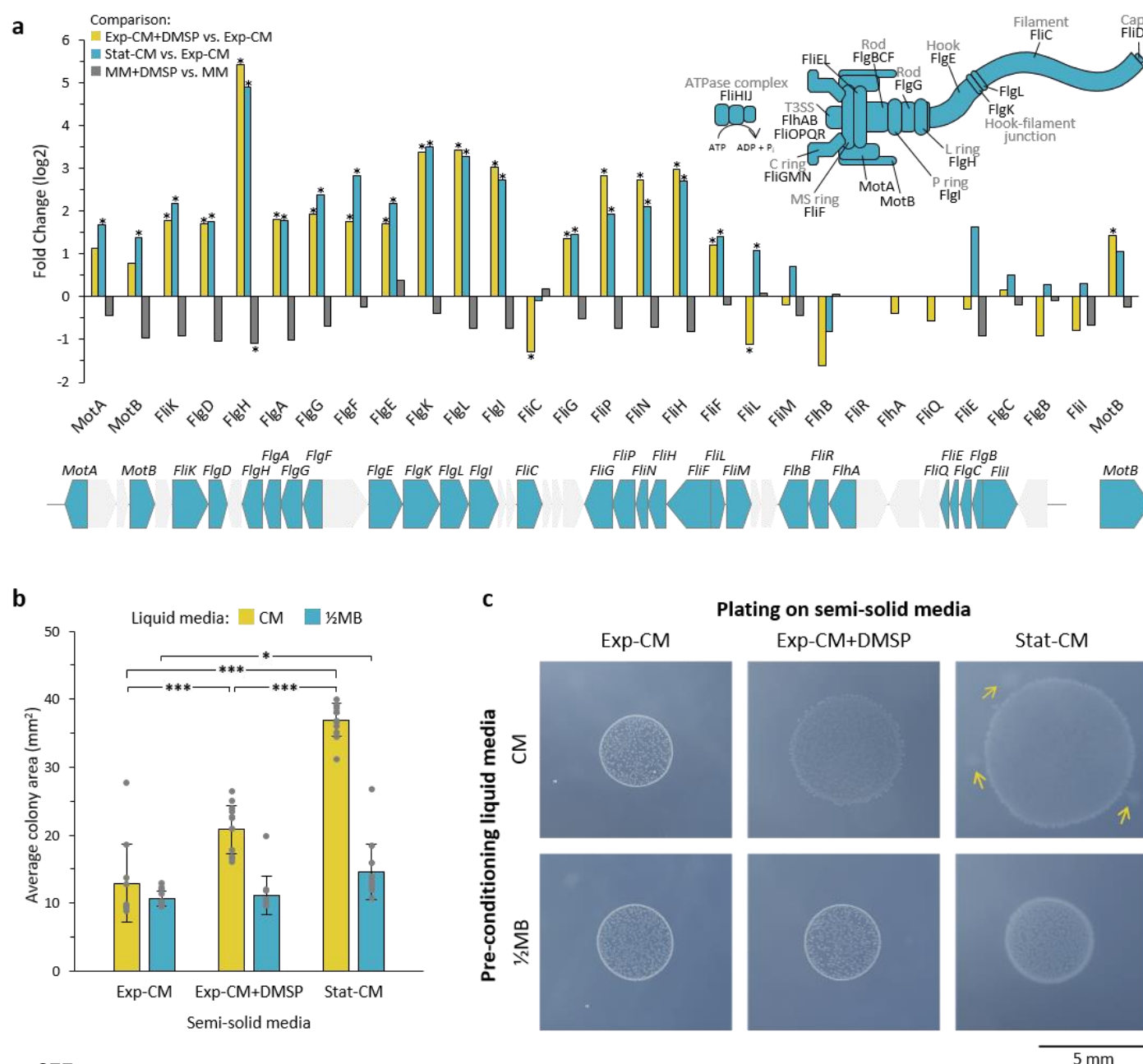
Fig. 2. Induction of flagellar genes and increased motility in pathogenicity-inducing media.
(a) Fold change of flagellar gene expression in the comparisons: Exp-CM+DMSP vs. Exp-CM (yellow), Stat-CM vs. Exp-CM (blue) and MM+DMSP vs. MM (grey). Genes marked with * are significantly DE. The flagellar genes are encoded on the *Sulfitobacter* D7 chromosome in an operon-like structure, as shown below the graph. Genes in grey are not related to the flagellum. The function of each gene is indicated in the flagellum assembly scheme on the top-right. Expression values are presented in Table S5. (b) Bacterial motility inferred by the colony area of *Sulfitobacter* D7 plated on semi-solid agar media (0.3% agarose). Bacteria were pre-conditioned in liquid CM (Exp-CM, Exp-CM+DMSP and Stat-CM) for 24 h and plated on the corresponding

27

887   semi-solid CM plates (yellow bars). For control, bacteria were pre-conditioned on ½MB and plated

888   on semi-solid CM plates (blue bars). Colony area was determined after 6 days of growth. Results

889   represent average ± SD (n=10-12 colonies per treatment). * P-value<0.05, *** P-value<0.0001. (c)

890   Representative bacterial colonies from each treatment showing the difference in colony area and

891   morphology. The arrows depict bacterial motility extensions from the core colony. The extensions

892   were not included in the colony area measurements.

893
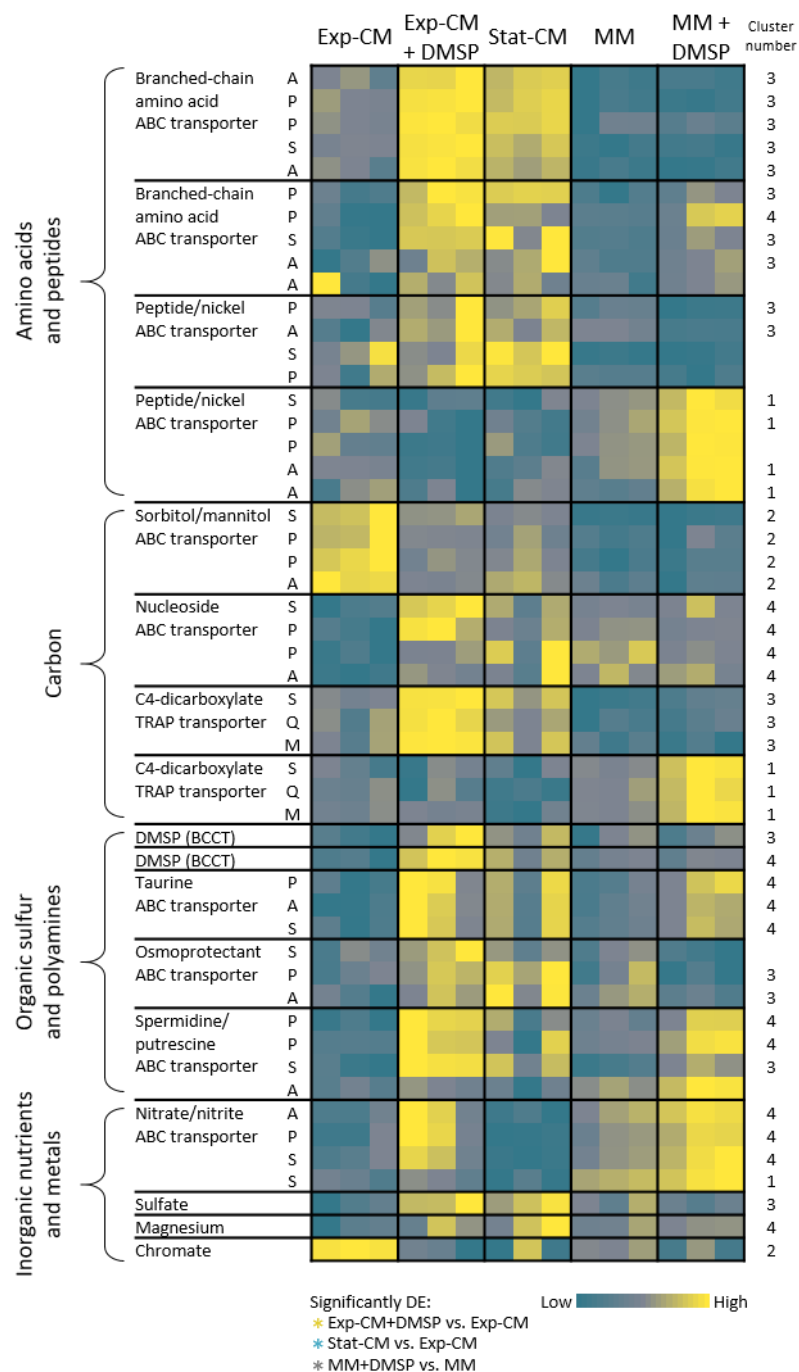
Fig. 3. **Remodeling of *Sulfitobacter* D7 transport systems in response to DMSP and *E. huxleyi*-derived metabolites.**

Heatmap of gene expression of representative transport genes for various metabolite classes. Each row represents one gene and the blocks represent a complete transport system in which at least two genes were DE in the comparisons indicated on the bottom. The column "cluster number" corresponds to the heatmap-cluster in Fig. 1d in which the gene is found. Colored * denote in which comparison the gene was significantly DE. Color intensity correspond to the standardized

29

901   expression across all samples (triplicates of each treatment are shown). Expression values are
902   scaled by row. Expression and fold-change values are presented in Table S6. ABC, ATP-binding
903   cassette; TRAP, tripartite ATP-independent periplasmic; BCCT, betaine/Carnitine/Choline
904   Transporter. The letters corresponds to the transport system components: A, ATP-binding; S,
905   substrate-binding; P, permease; Q, dctQ subunit; M, dctM subunit.

a

COO⁻

Benzoate

BenABC

1,2-*cis*-dihydroxybenzoate

BenD

Catechol

CatA

cis,cis-muconate

CatB
PcaD

β-ketoadipate

Succinyl-CoA

PcaIJ

β-ketoadipyl-CoA

PcaF

Succinate   Acetyl-CoA

b

Treatment:
- Exp-CM
- Exp-CM+DMSP
- Stat-CM
- MM
- MM+DMSP

Expression values (log transformed)
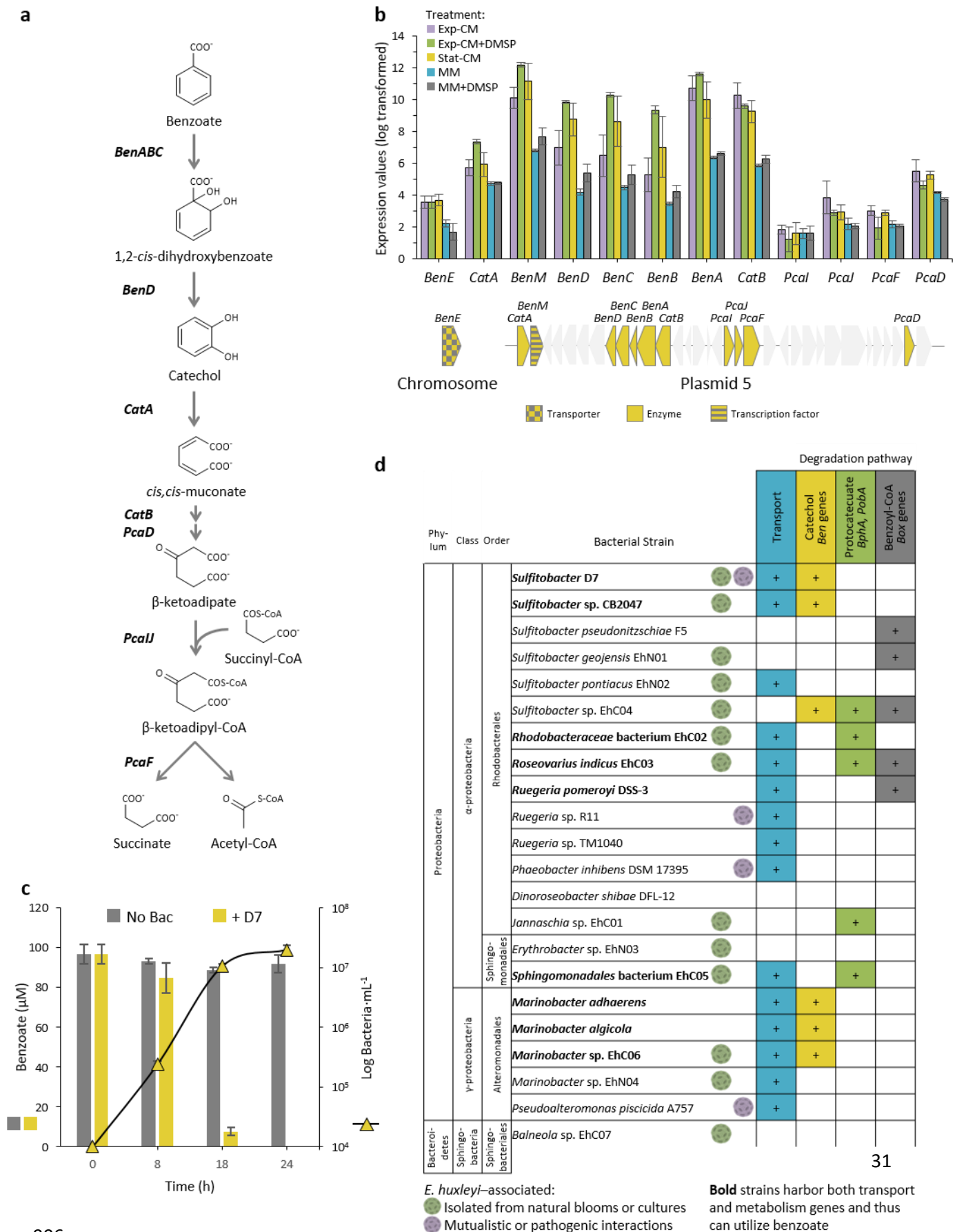
BenE *CatA* *BenM* *BenD* *BenC* *BenB* *BenA* *CatB* *PcaI* *PcaJ* *PcaF* *PcaD*

BenE   *BenM CatA*   *BenC BenA / BenD BenB CatB*   *PcaJ PcaI PcaF*   *PcaD*

Chromosome   Plasmid 5

Transporter   Enzyme   Transcription factor

c

No Bac   + D7

Benzoate (μM) / Log Bacteria·mL⁻¹

Time (h)

d

Degradation pathway

Phy-lum	Class	Order	Bacterial Strain			Transport	Catechol *Ben* genes	Protocatecuate *BphA, PobA*	Benzoyl-CoA *Box* genes
Proteobacteria	α-proteobacteria	Rhodobacterales	**Sulfitobacter D7**	🟢	🟣	+	+		
			Sulfitobacter sp. CB2047	🟢		+	+		
			Sulfitobacter pseudonitzschiae F5						+
			Sulfitobacter geojensis EhN01	🟢					+
			Sulfitobacter pontiacus EhN02	🟢		+			
			Sulfitobacter sp. EhC04	🟢			+	+	+
			Rhodobacteraceae bacterium EhC02	🟢		+		+	
			Roseovarius indicus EhC03	🟢		+		+	+
			Ruegeria pomeroyi DSS-3			+			+
			Ruegeria sp. R11		🟣	+			
			Ruegeria sp. TM1040			+			
			Phaeobacter inhibens DSM 17395		🟣	+			
			Dinoroseobacter shibae DFL-12						
			Jannaschia sp. EhC01	🟢				+	
	Sphingo-monadales		Erythrobacter sp. EhN03	🟢					
			Sphingomonadales bacterium EhC05	🟢		+		+	
	γ-proteobacteria	Alteromonadales	**Marinobacter adhaerens**			+	+		
			Marinobacter algicola			+	+		
			Marinobacter sp. EhC06	🟢		+	+		
			Marinobacter sp. EhN04	🟢		+			
			Pseudoalteromonas piscicida A757		🟣	+			
Bacteroidetes	Sphingo-bacteria	Sphingo-bacteriales	Balneola sp. EhC07	🟢					

E. huxleyi–associated:
🟢 Isolated from natural blooms or cultures
🟣 Mutualistic or pathogenic interactions

Bold strains harbor both transport and metabolism genes and thus can utilize benzoate

907 **Fig. 4.** *Sulfitobacter* **D7 encodes for a benzoate degradation pathway required for the**
908 **metabolic exchange with *E. huxleyi*.**
909 (a) The benzoate degradation pathway in *Sulfitobacter* D7. The genes that encode for the enzymes
910 mediating the subsequent transformations of benzoate to succinate and acetyl-CoA are denoted in
911 bold. (b) Expression values of benzoate-related genes, which are encoded on *Sulfitobacter* D7
912 plasmid 5 in an operon-like structure, as indicated below the graph. The benzoate transporter,
913 *BenE*, is encoded on the chromosome. Genes in grey are not related to benzoate. Results
914 represent average ± SD (n = 3). (c) Benzoate concentration (bars, left axis) and bacterial growth
915 (triangles, right axis) in MM supplemented with 100 µM benzoate, as a sole carbon source, without
916 inoculation (grey) and upon inoculation of *Sulfitobacter* D7 (yellow). Results represent average ±
917 SD (n = 3). *P*-value<0.0001 for the difference in benzoate concentration between the "No bac" and
918 "+D7" treatments. No bacterial growth was observed in un-inoculated MM. (d) Presence of
919 benzoate transport and degradation genes in genomes of phytoplankton-associated bacteria. *E.*
920 *huxleyi*-associated bacteria are denoted. Colored tiles depict the presence of the genes. Bacterial
921 strains highlighted in bold possess genes for both transport and degradation of benzoate. Bacterial
922 benzoate degradation pathways are elaborated in Fig. S3. The full data of the presence of all query
923 genes in the genomes of the bacteria is presented in Table S9. The query genes are listed in Table
924 S10. *BenABC*, benzoate 1,2-dioxygenase subunit alpha, beta and reductase component,
925 respectively; *BenD*, *cis*-1,2-dihydroxybenzoate dehydrogenase; *CatA*, catechol 1,2-dioxygenase;
926 *CatB*, muconate cycloisomerase; *PcaD*, 3-oxoadipate enol-lactonase; *PcaIJ,* 3-oxoadipate CoA-
927 transferase, alpha and beta subunits, respectively; *PcaF*, 3-oxoadipyl-CoA thiolase.
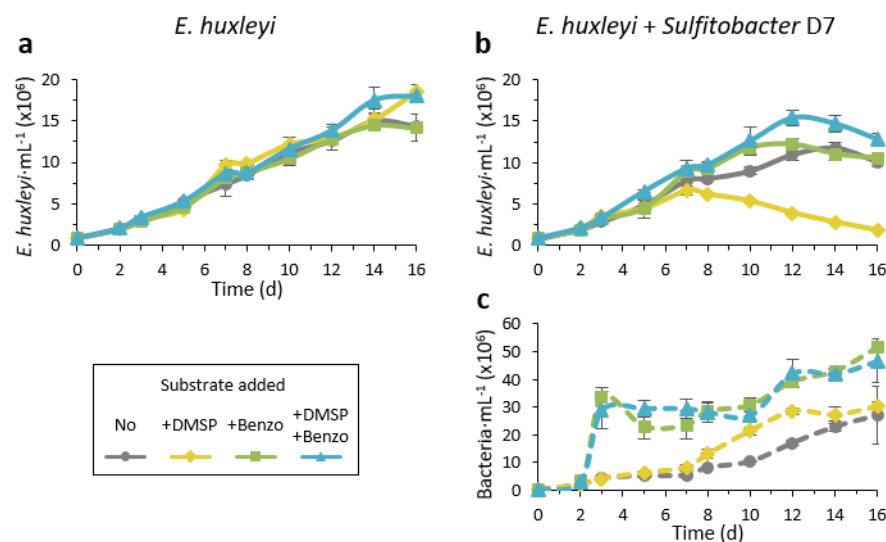
Fig. 5. **Benzoate is a key metabolite for maintaining *E. huxleyi-Sulfitobacter* D7 coexistence.** Time course of *E. huxleyi* (strain CCMP2090) and bacterial abundance (smooth and dashed lines, respectively) in algal mono-cultures (a) or during co-culturing with *Sulfitobacter* D7 (b-c). No bacterial growth was observed in algal mono-cultures. Cultures were supplemented at day 0 with 100 μM of DMSP (yellow), benzoate (benzo, green), DMSP and benzoate (blue) or none (grey). The presence of benzoate negated the pathogenicity-inducing effect of DMSP. Results represent average ± SD (n = 3). *P*-value<0.0001 for the difference in *E. huxleyi* growth in the treatment of "+D7+DMSP" compared to all other treatments. *P*-value<0.05 for the differences in bacterial growth in the treatments "+D7+benzoate" and "+D7+Benzoate+DMSP" compared to only "+D7". *P*-values for all comparisons are listed in Table S11.
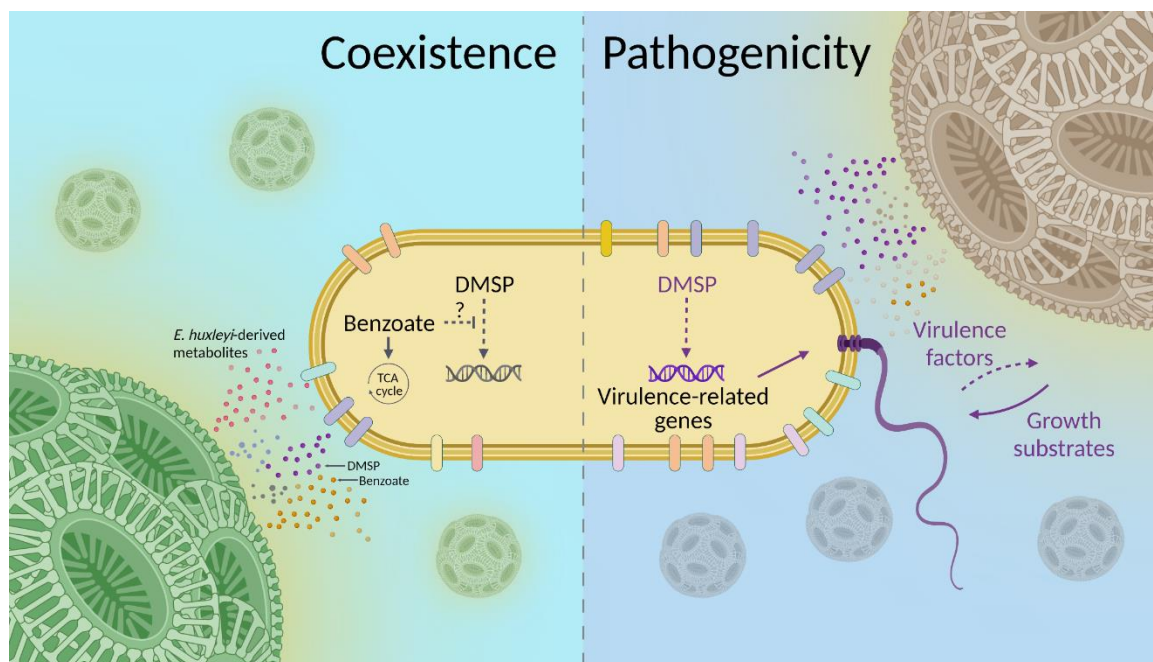
Fig. 6. Conceptual model of the lifestyle switch of *Sulfitobacter* D7 in response to *E. huxleyi*-derived metabolites.

During its interactions with *E. huxleyi*, *Sulfitobacter* D7 exhibits a lifestyle switch from coexistence to pathogenicity. In the coexistence phase, *E. huxleyi* secretes to the phycosphere various metabolites such as benzoate, DMSP and other growth substrates, which bacteria can uptake and consume for growth. Based on the observation that benzoate negated the pathogenicity-inducing effect of DMSP, we hypothesize that such energy-rich metabolic currencies hinder DMSP signaling in *Sulfitobacter* D7. When the algal physiological state is compromised, e.g. stationary growth, the amount of available growth substrates decreases, due to bacterial consumption and less secretion by the alga. In this context, high concentration of algal DMSP acts as a signal that alters the transcriptional profiles of the bacterium and leads to high expression of pathogenicity-related genes such as flagellar and transport genes, and yet unknown virulence factors that kill *E. huxleyi* cells. This leads to a surge of alga-derived growth substrates that are taken up efficiently by *Sulfitobacter* D7. The flagellum can mediate the dispersal of *Sulfitobacter* D7 and to forage for an alternative host.